



*Supplement of*

## **Extensional exhumation of cratons: insights from the Early Cretaceous Rio Negro–Juruena belt (Amazonian Craton, Colombia)**

**Ana Fonseca et al.**

*Correspondence to:* Ana Fonseca ([anacarolina.liberalfonseca@ugent.be](mailto:anacarolina.liberalfonseca@ugent.be))

The copyright of individual parts of the supplement might differ from the article licence.

## S1: Radial plots

The radial plot was introduced as a more appropriate data visualisation tool for showcasing single grain age AFT data dispersion (**Galbraith, 1988, 1990**), by mapping  $y$  against  $x$ , with:

$$x_j = 1/\sigma_j$$

$$y_j = (A_j - A_r)/\sigma_j,$$

where  $\sigma_j$  is the precision of the age estimate  $A_j$ , and  $A_r$  is some reference age (typically the mean age of all grains).

On a radial plot, the more precise data plot farther from the origin, all data have a common normalized error, and a line joining a given data point to the origin has a slope ( $y/x$ ) equivalent to the age (or age-reference age). Consequently, the plot exhibits distinct patterns: a line from the origin indicates a constant fission track age, and the precision of each grain age is indicated by the  $x$  value. This layout allows for the identification of precise grains on the right side of the plot (high  $x$ , low error). The age scale, delineated radially around the plot's perimeter in millions of years, provides a comprehensive view of age distribution. Any deviation of data points beyond certain limits (+2 and -2 standard deviations) signifies a considerable spread in individual grain ages, corroborated by indicators of age dispersion.

Galbraith RF. 1988. Graphical display of estimates having different standard errors. *Technometrics* 30:271–81

Galbraith RF. 1990. The radial plot: graphical assessment of spread in ages. *Nucl. Tracks* 17:207–14

**Figure S1.** Radial plot for sample 171, constructed using QTQt (Gallagher, 2012).

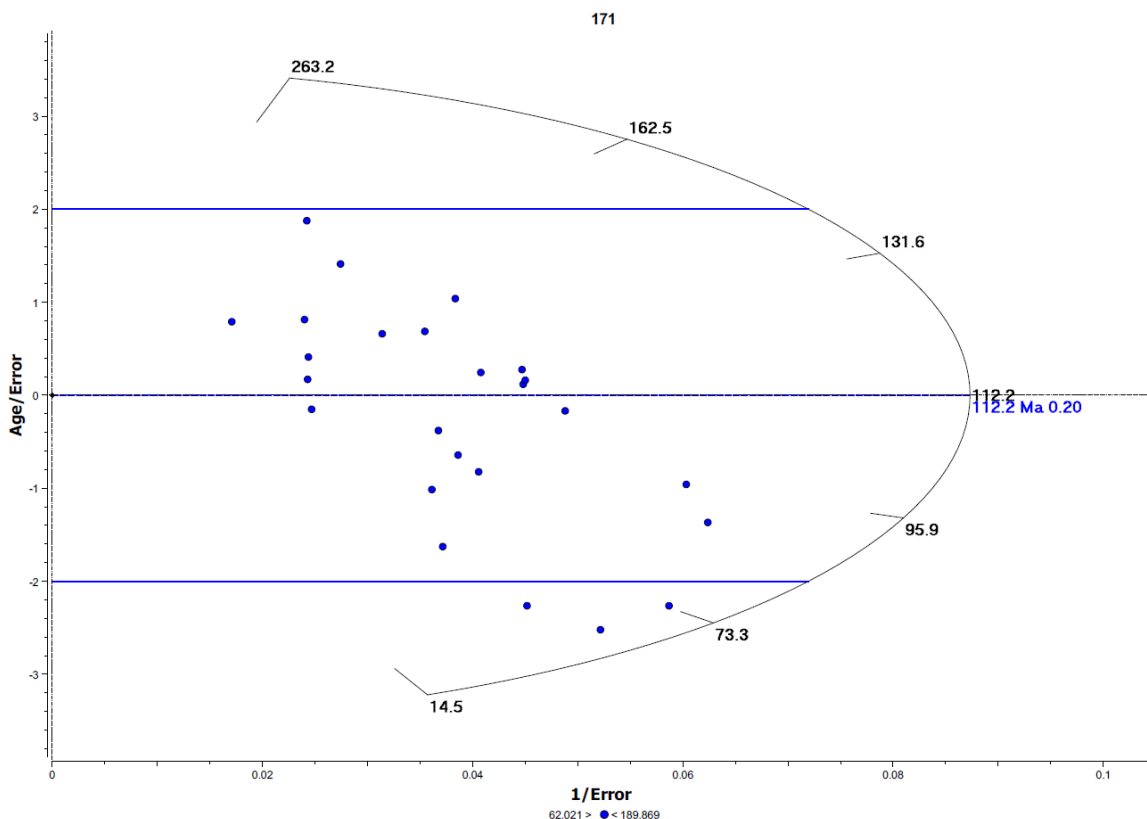


**Figure S2.** Radial plot for sample 175, constructed using QTQt (Gallagher, 2012).

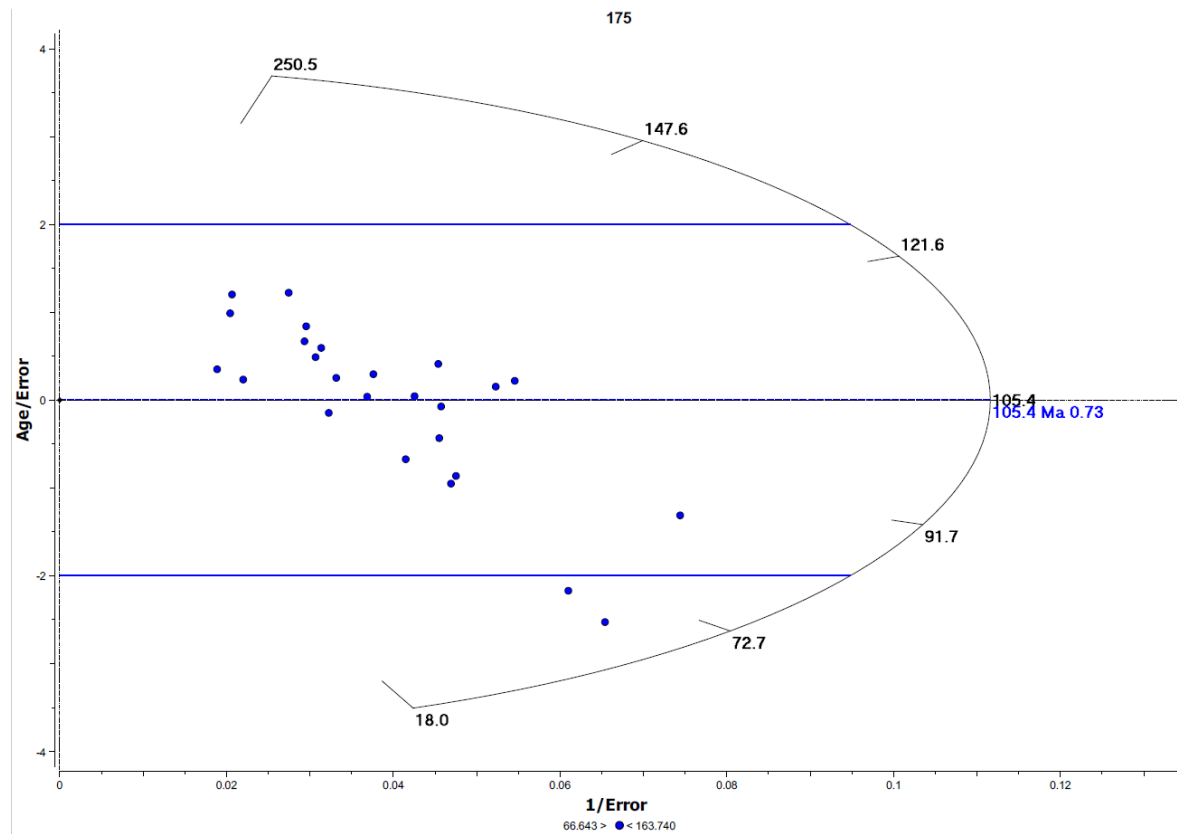


**Figure S3.** Radial plot for sample 176, constructed using QTQt (Gallagher, 2012).

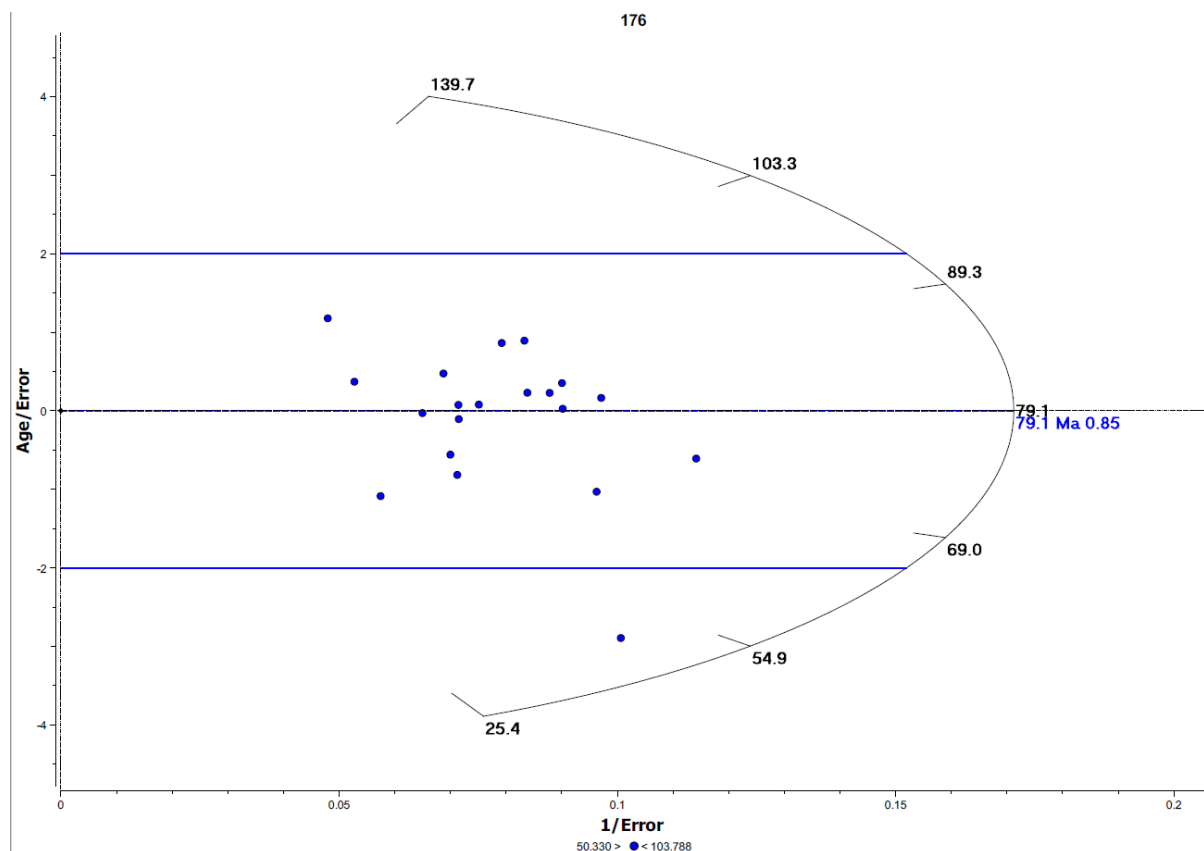


**Figure S4.** Radial plot for sample 180, constructed using QTQt (Gallagher, 2012).

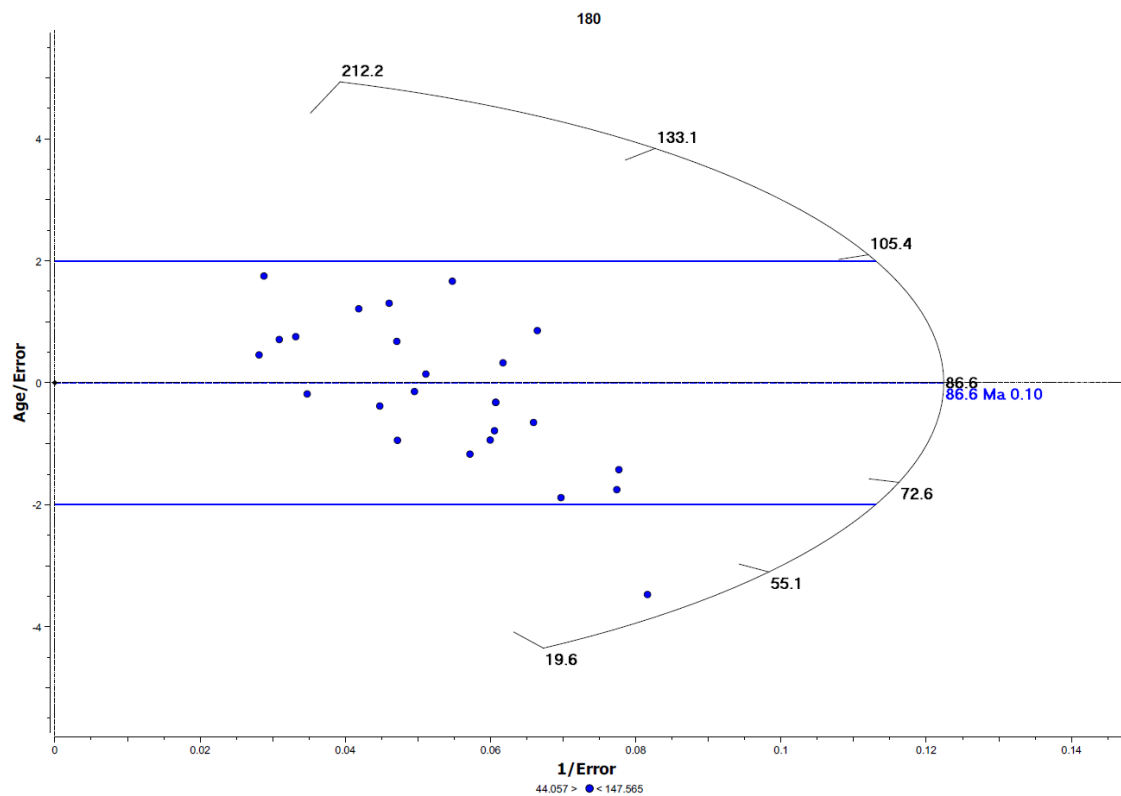


**Figure S5.** Radial plot for sample 182, constructed using QTQt (Gallagher, 2012).

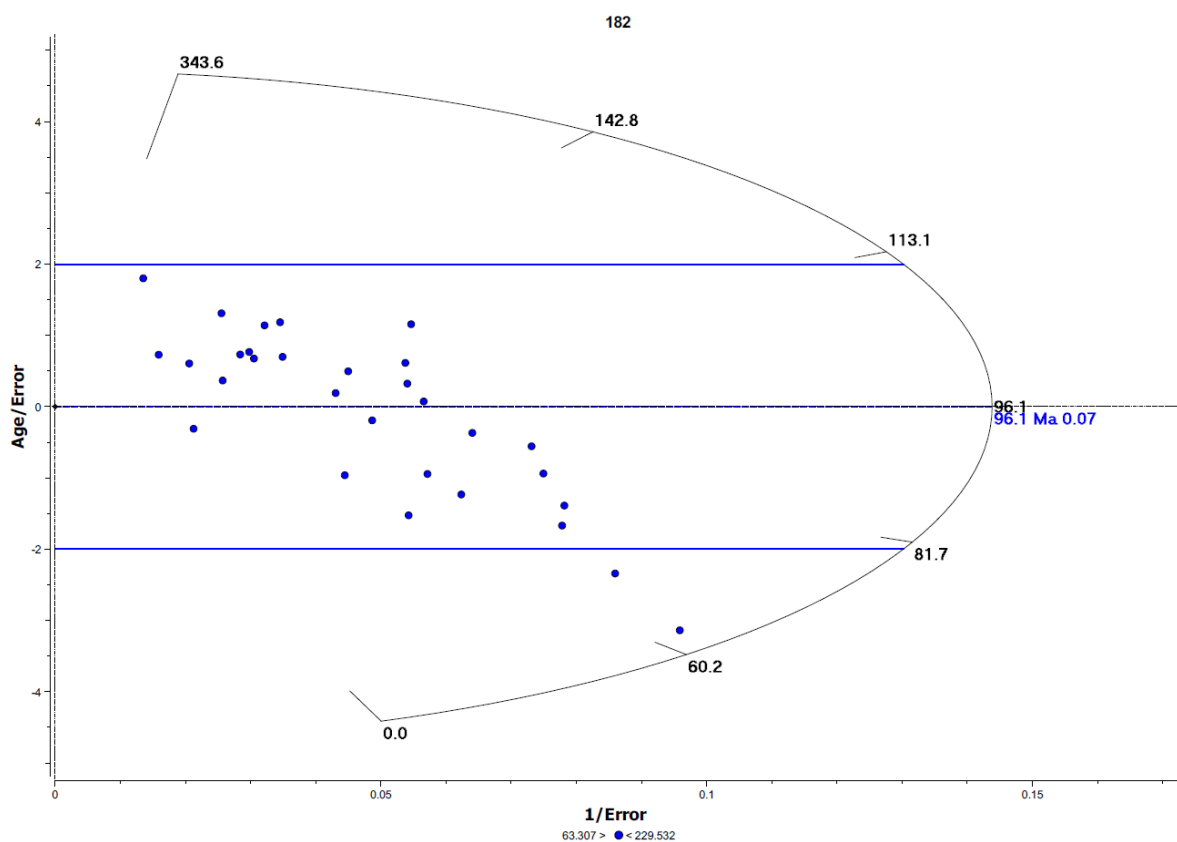


**Figure S.6.** Radial plot for sample 164, constructed using QTQt (Gallagher, 2012).

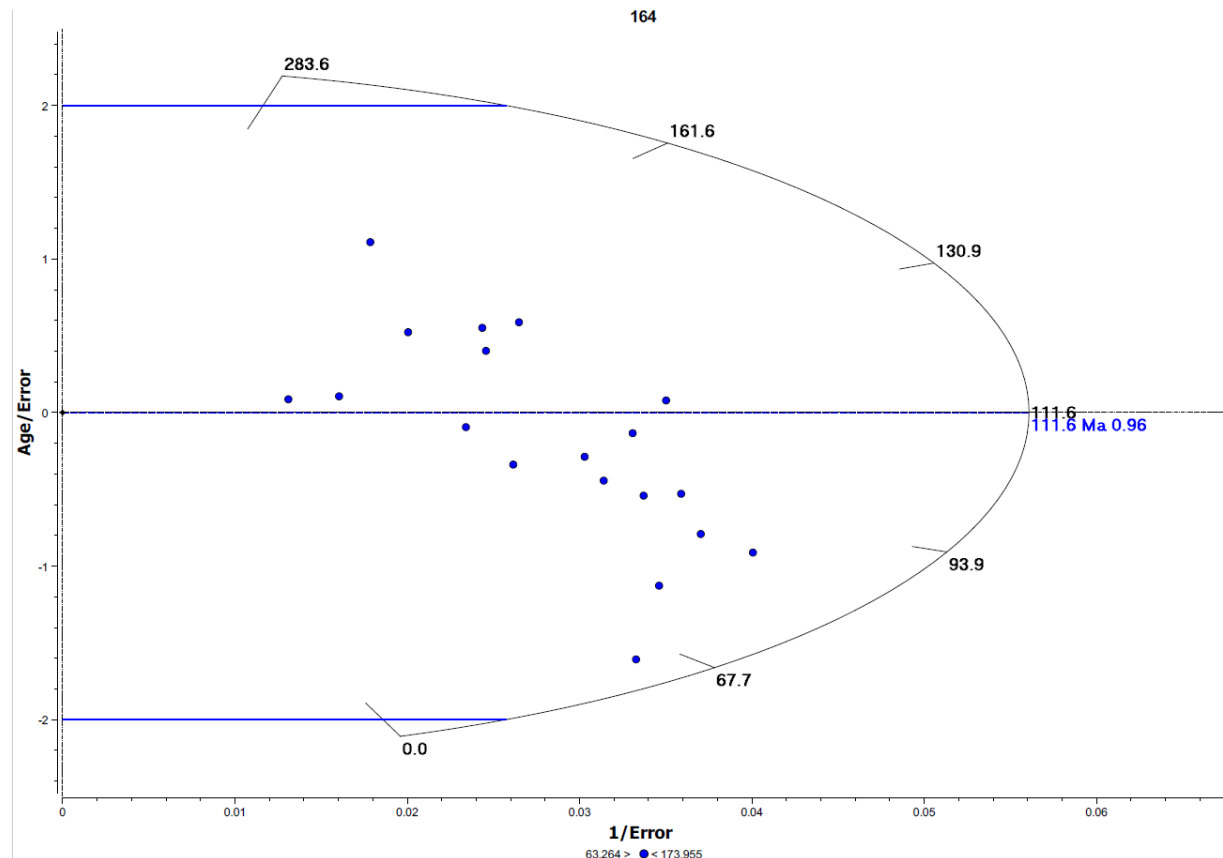


**Figure S.7.** Radial plot for sample 168, constructed using QTQt (Gallagher, 2012).

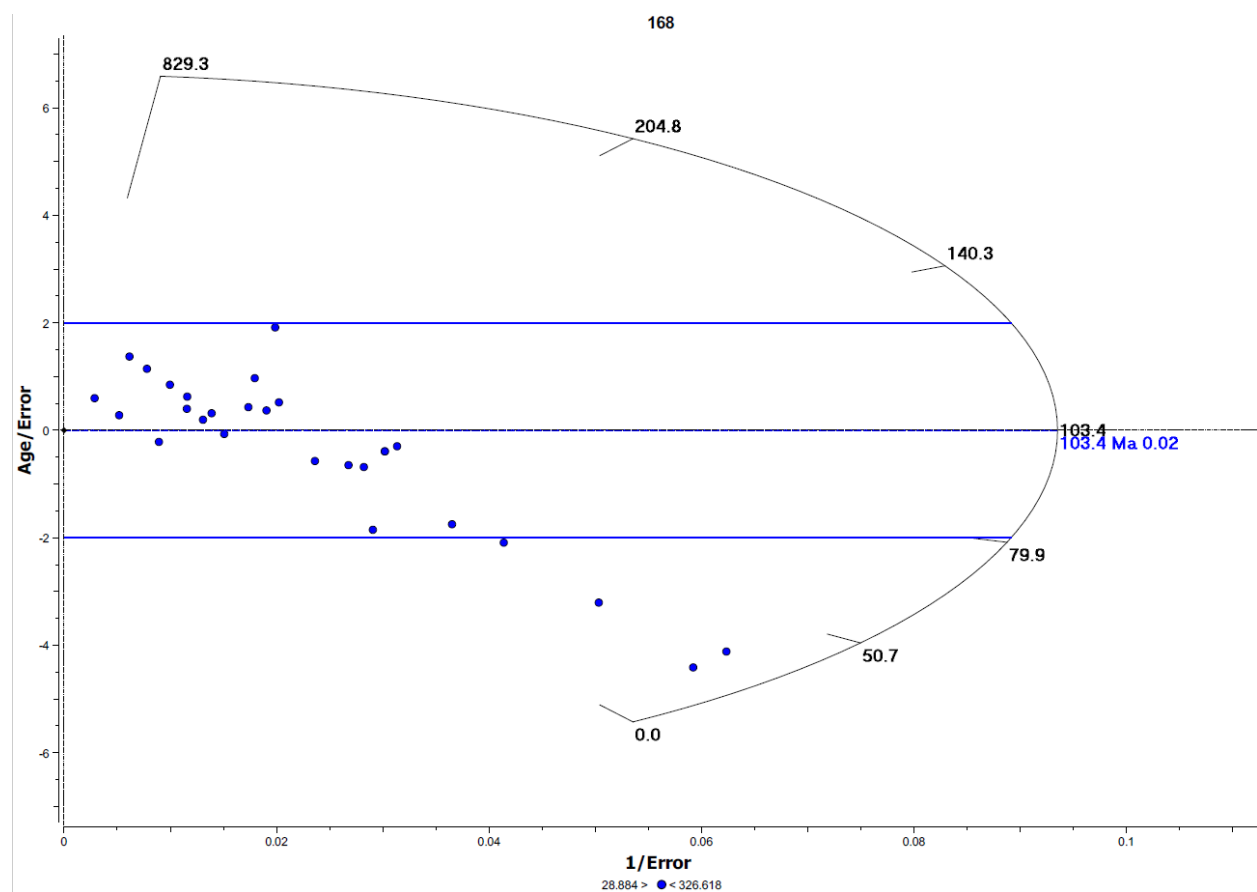


**Figure S.8.** Radial plot for sample 170, constructed using QTQt (Gallagher, 2012).

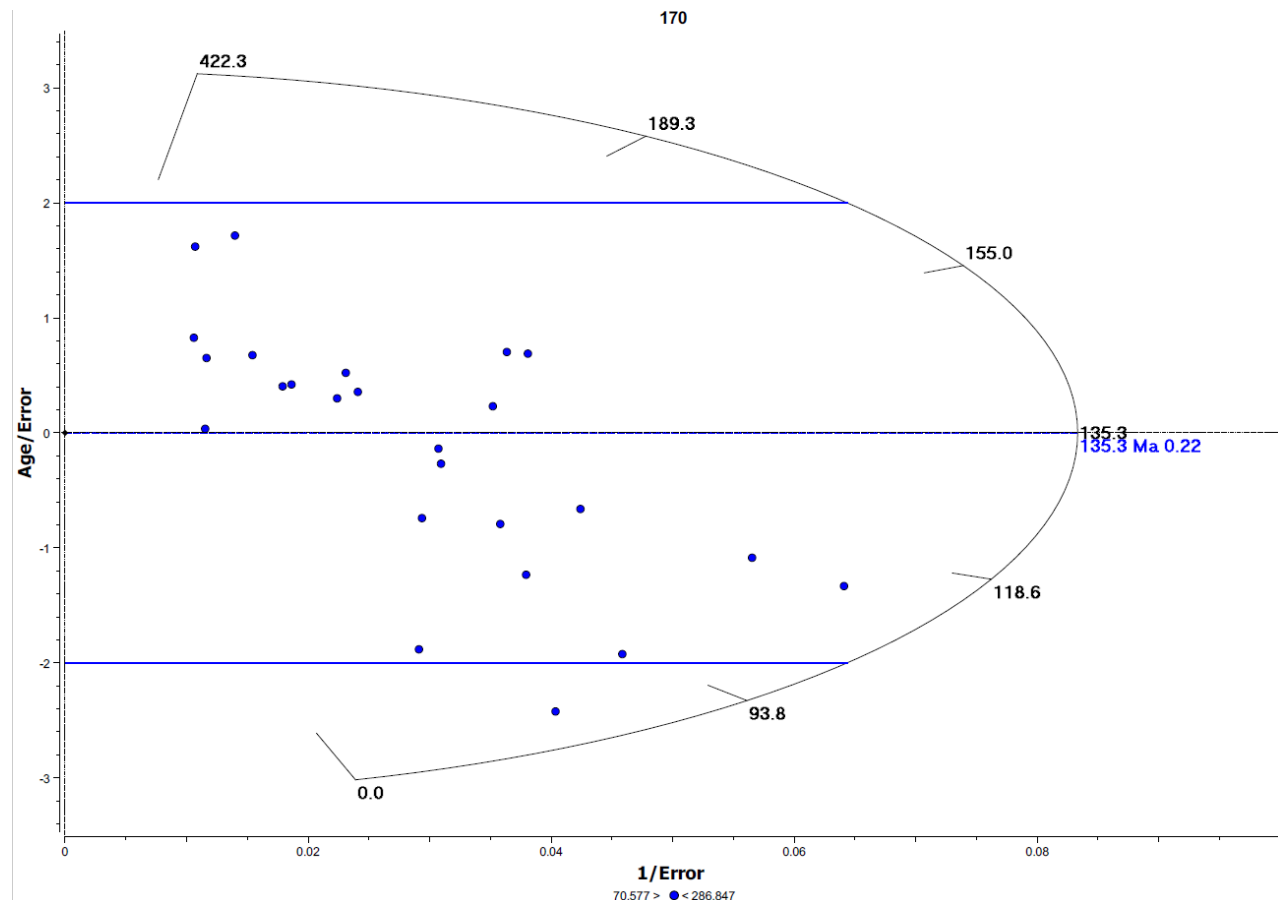


**Figure S.9.** Radial plot for sample 501, constructed using QTQt (Gallagher, 2012).

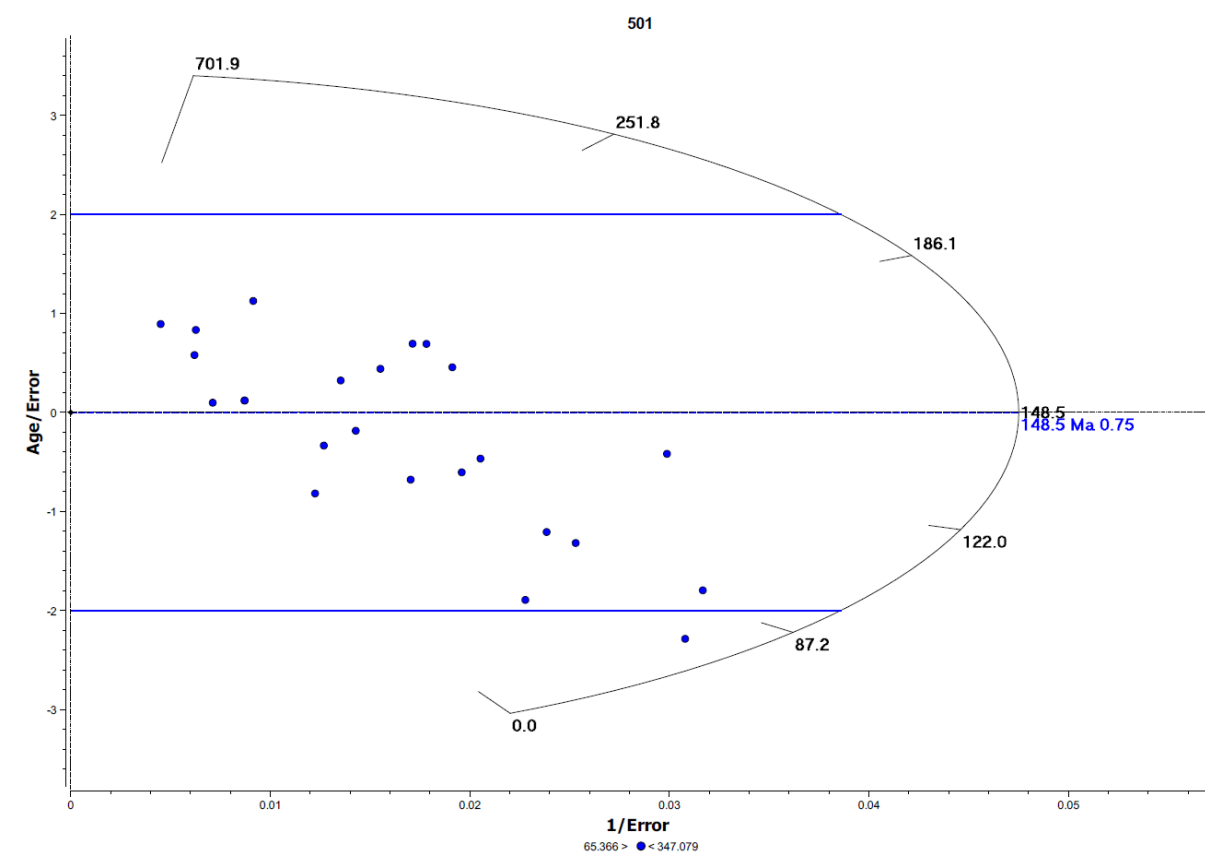


**Figure S.10.** Radial plot for sample 502, constructed using QTQt (Gallagher, 2012).

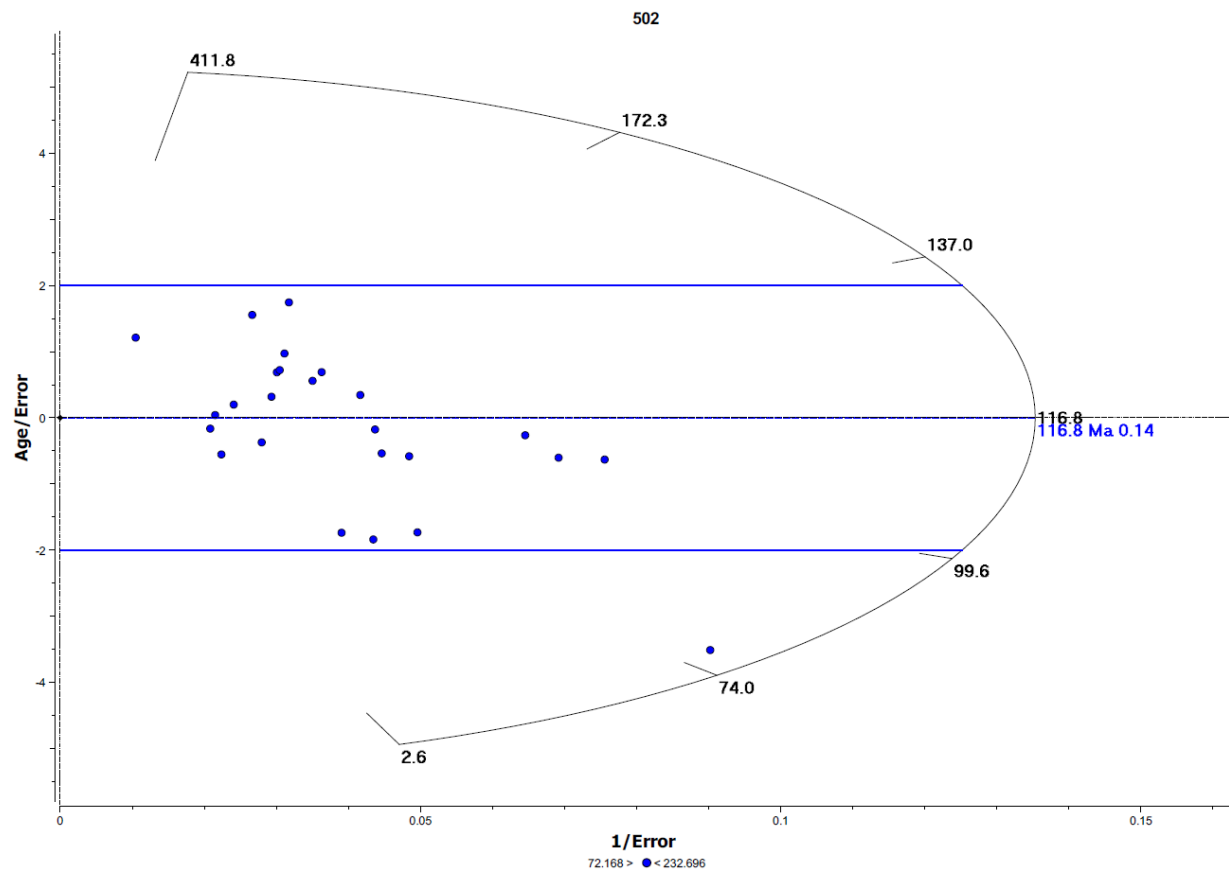


**Figure S.11.** Radial plot for sample 505, constructed using QTQt (Gallagher, 2012).

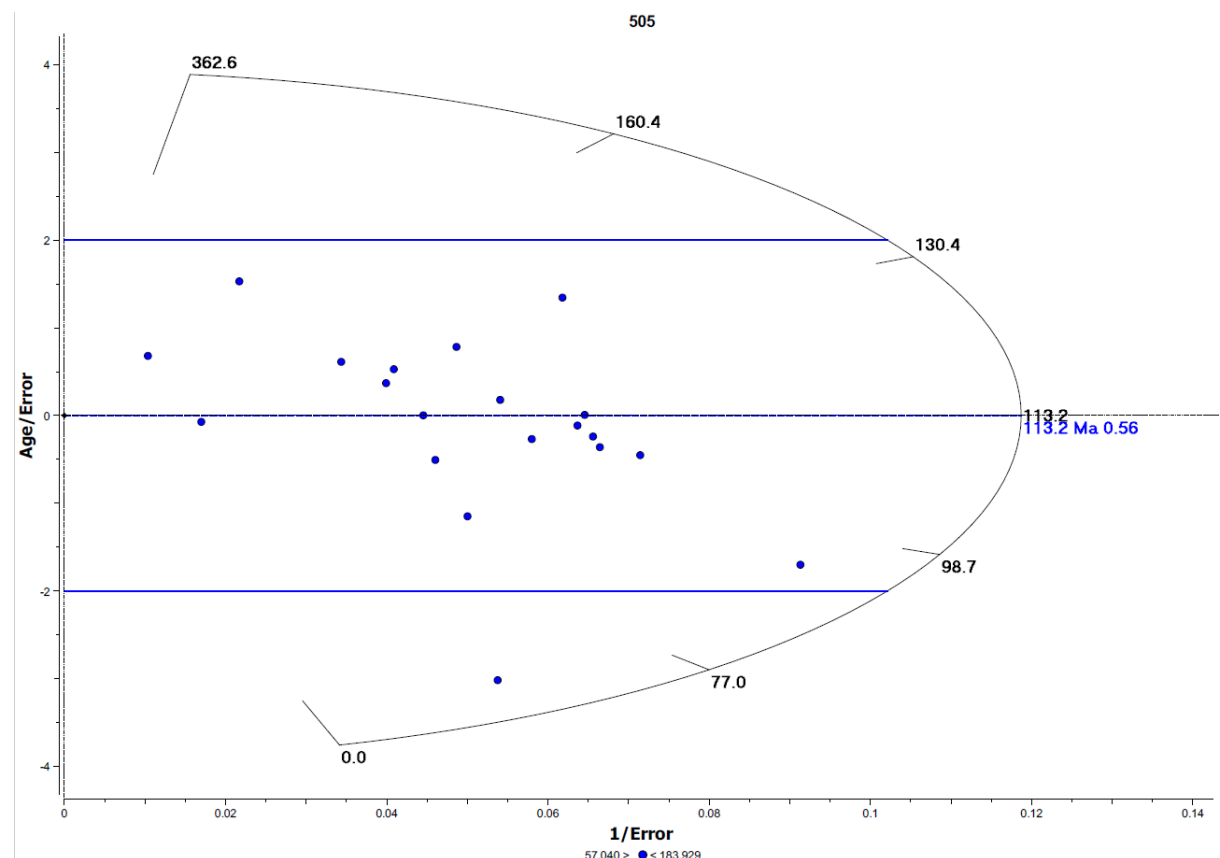


**Figure S.12.** Radial plot for sample 506, constructed using QTQt (Gallagher, 2012).

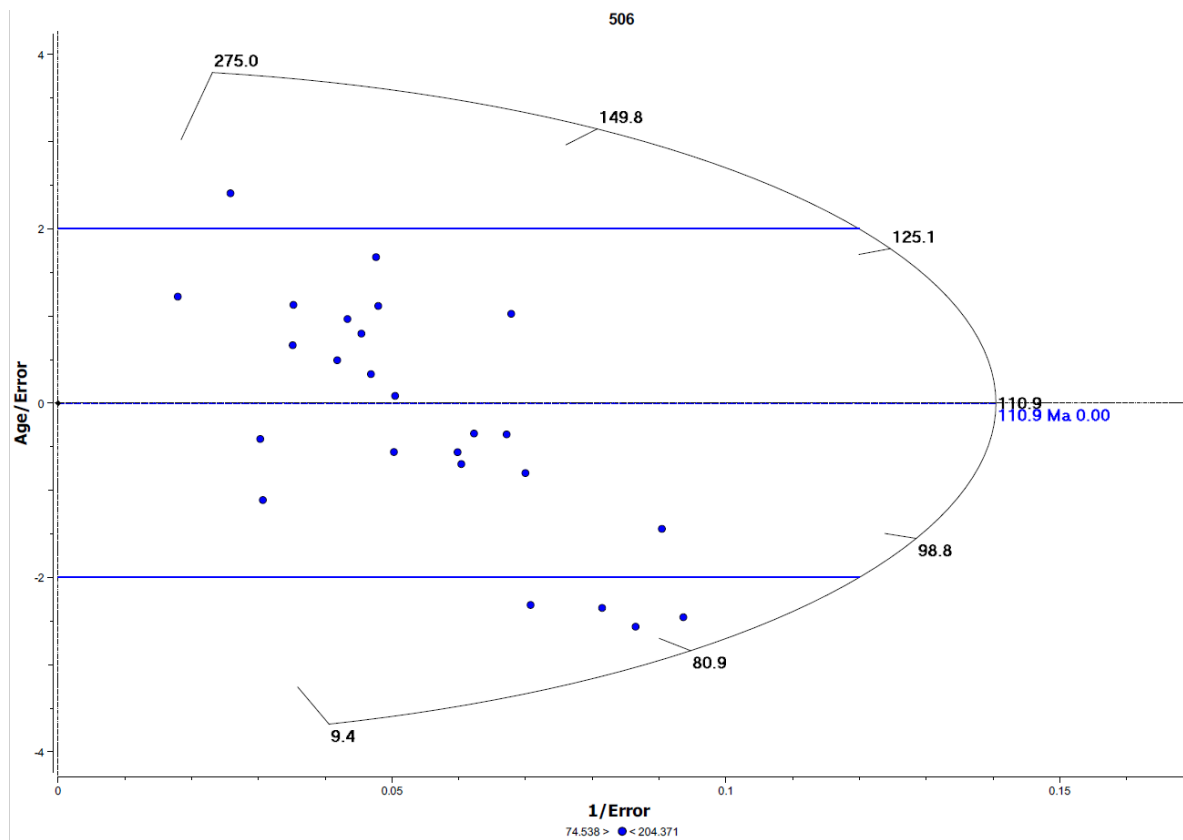


**Figure S.13.** Radial plot for sample 510, constructed using QTQt (Gallagher, 2012).

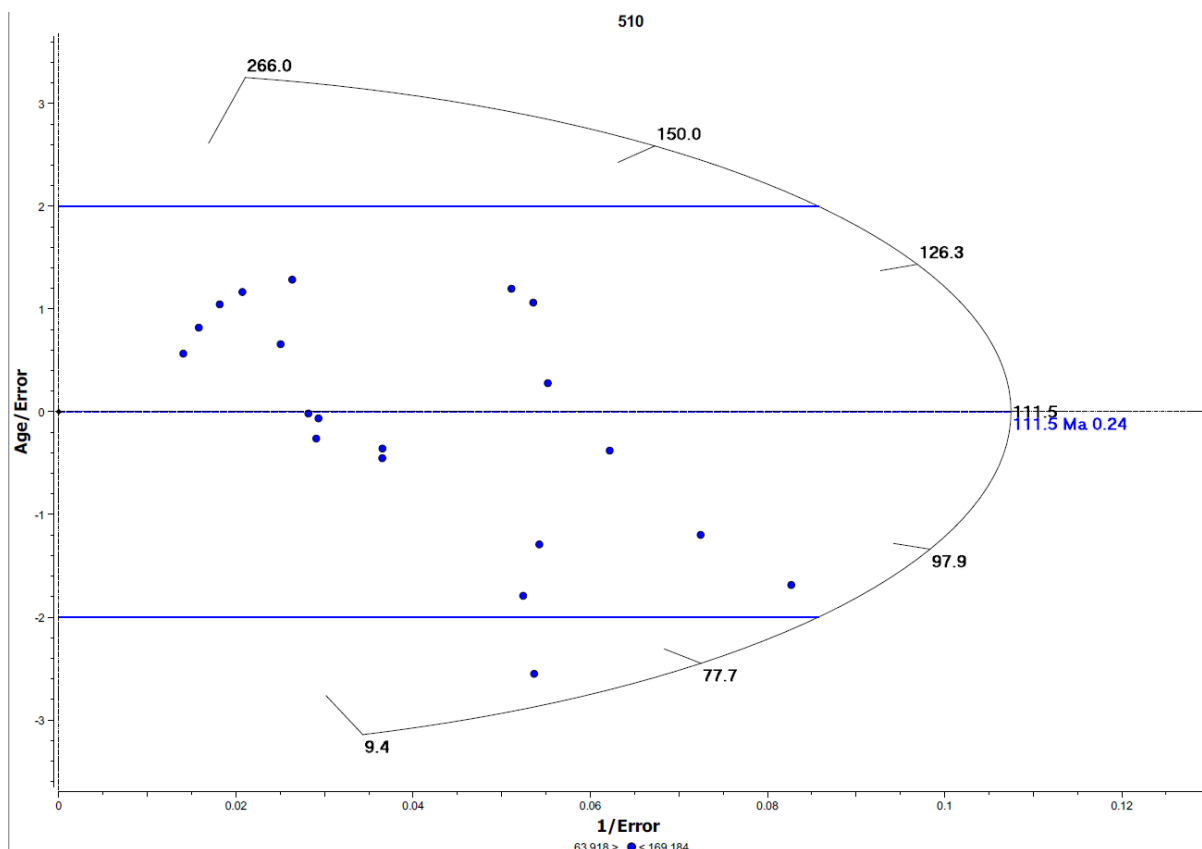


**Figure S.14.** Radial plot for sample 512, constructed using QTQt (Gallagher, 2012).

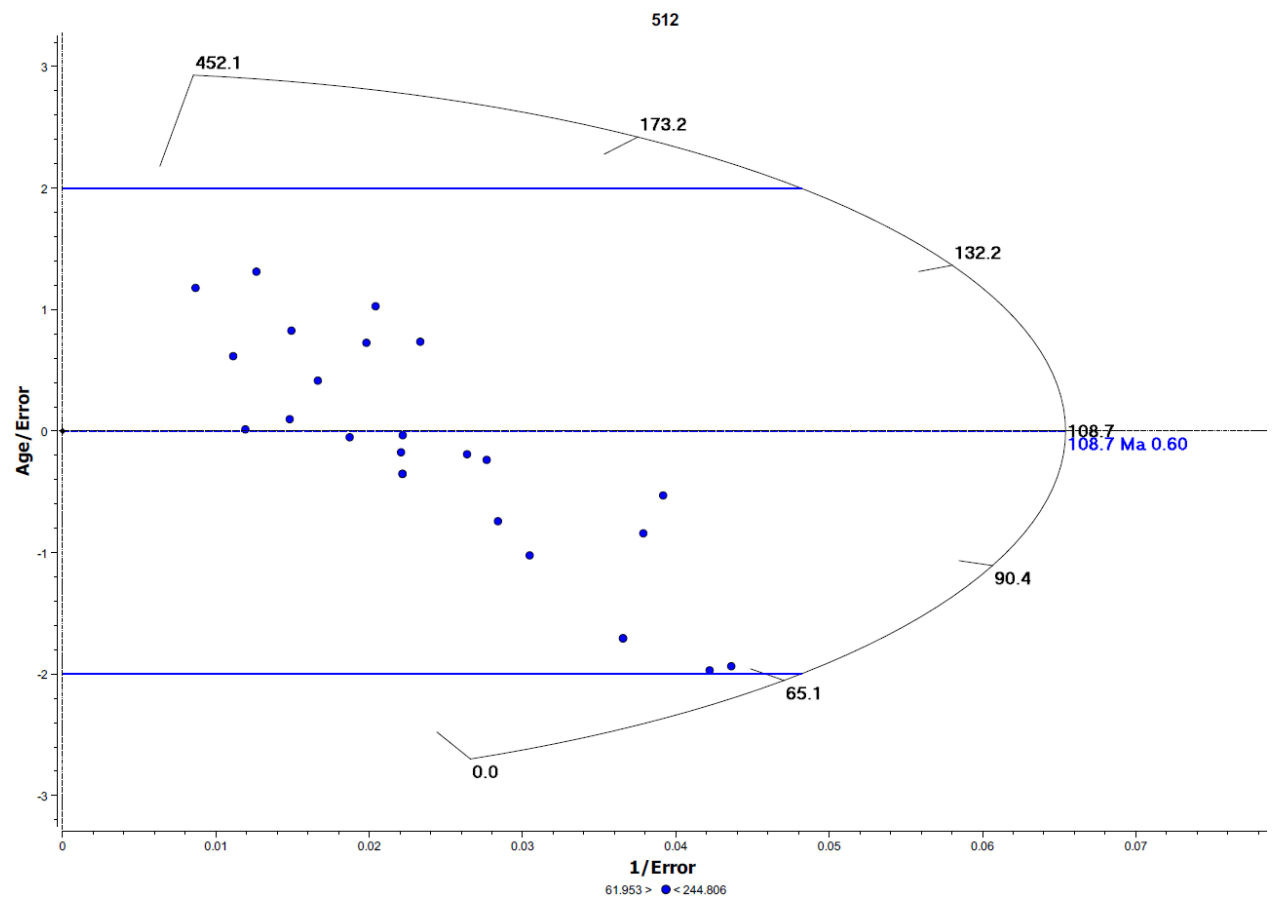


**Figure S.15.** Radial plot for sample 515, constructed using QTQt (Gallagher, 2012).

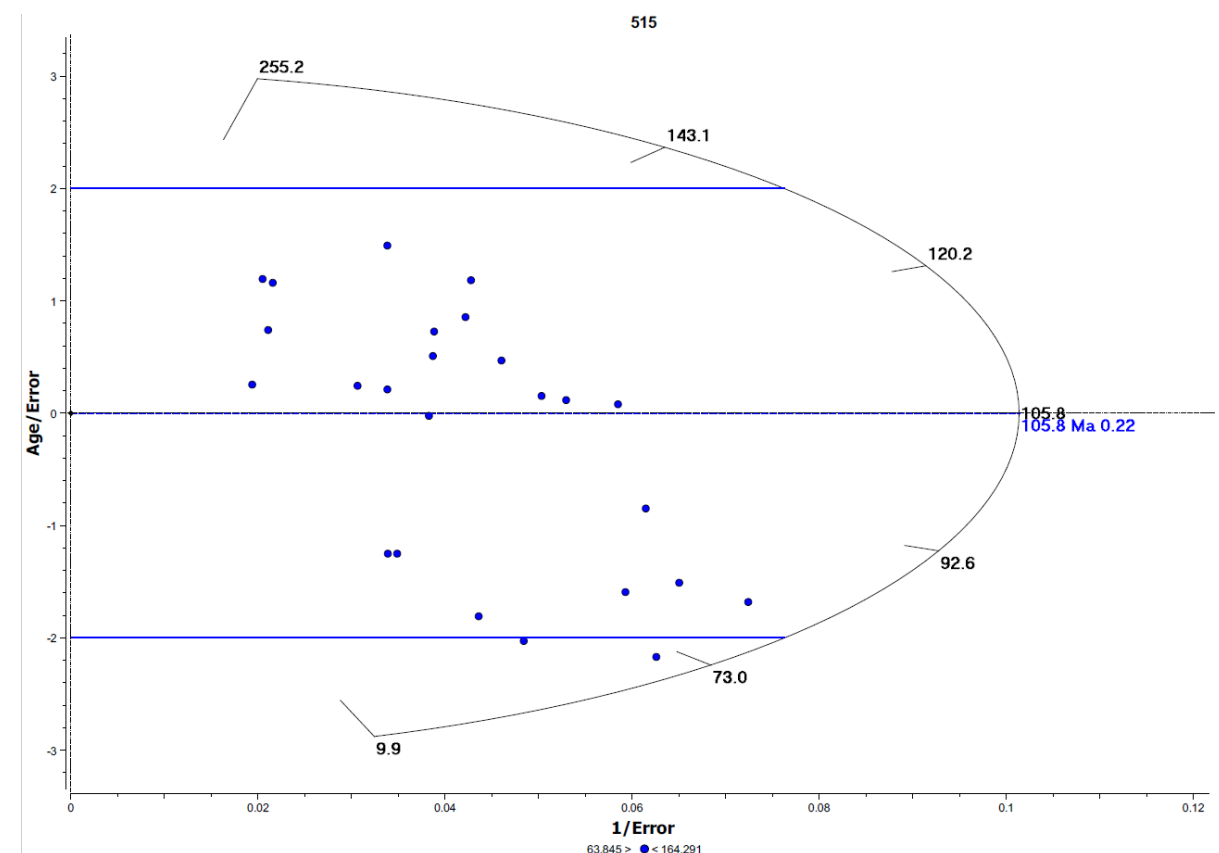


**Figure S.16.** Radial plot for sample 516, constructed using QTQt (Gallagher, 2012).

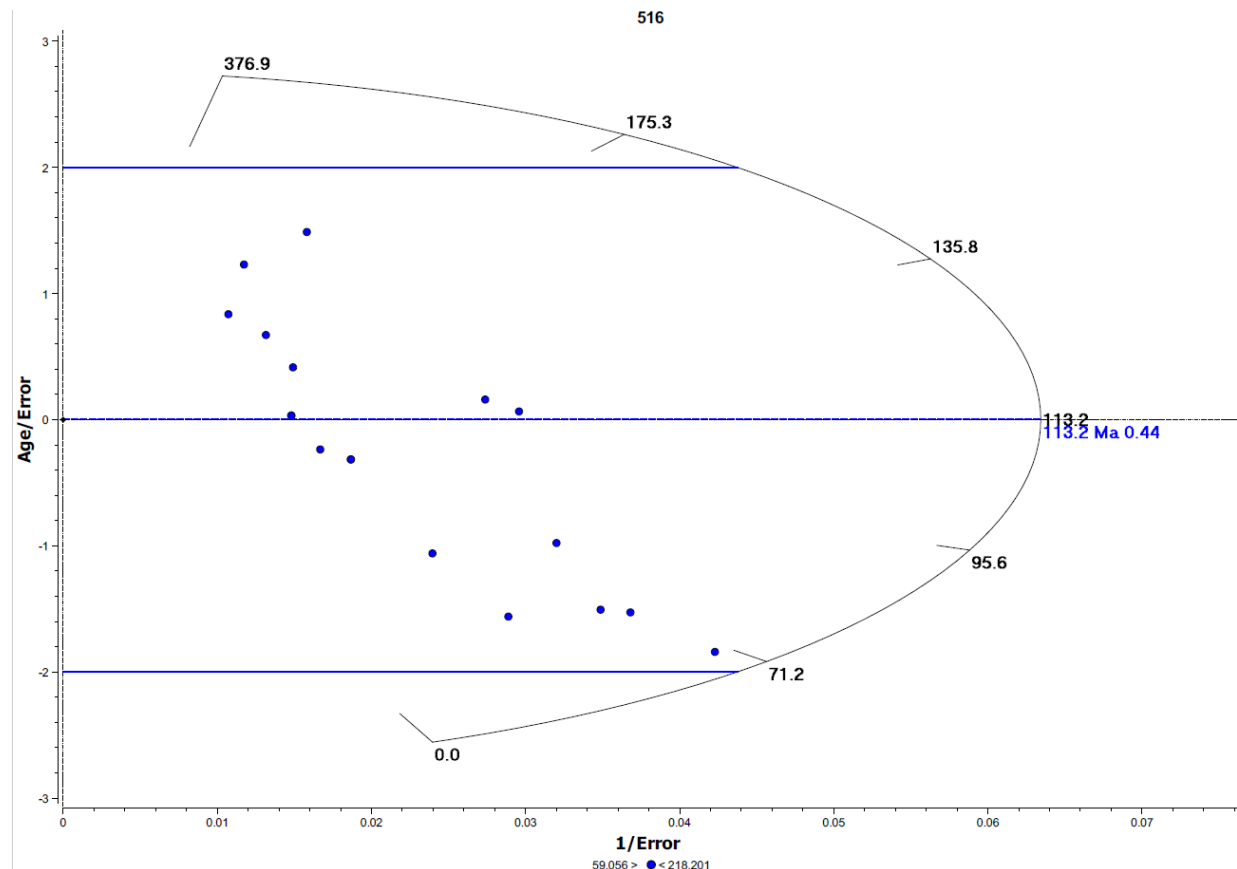


**Figure S.17.** Radial plot for sample 192, constructed using QTQt (Gallagher, 2012).

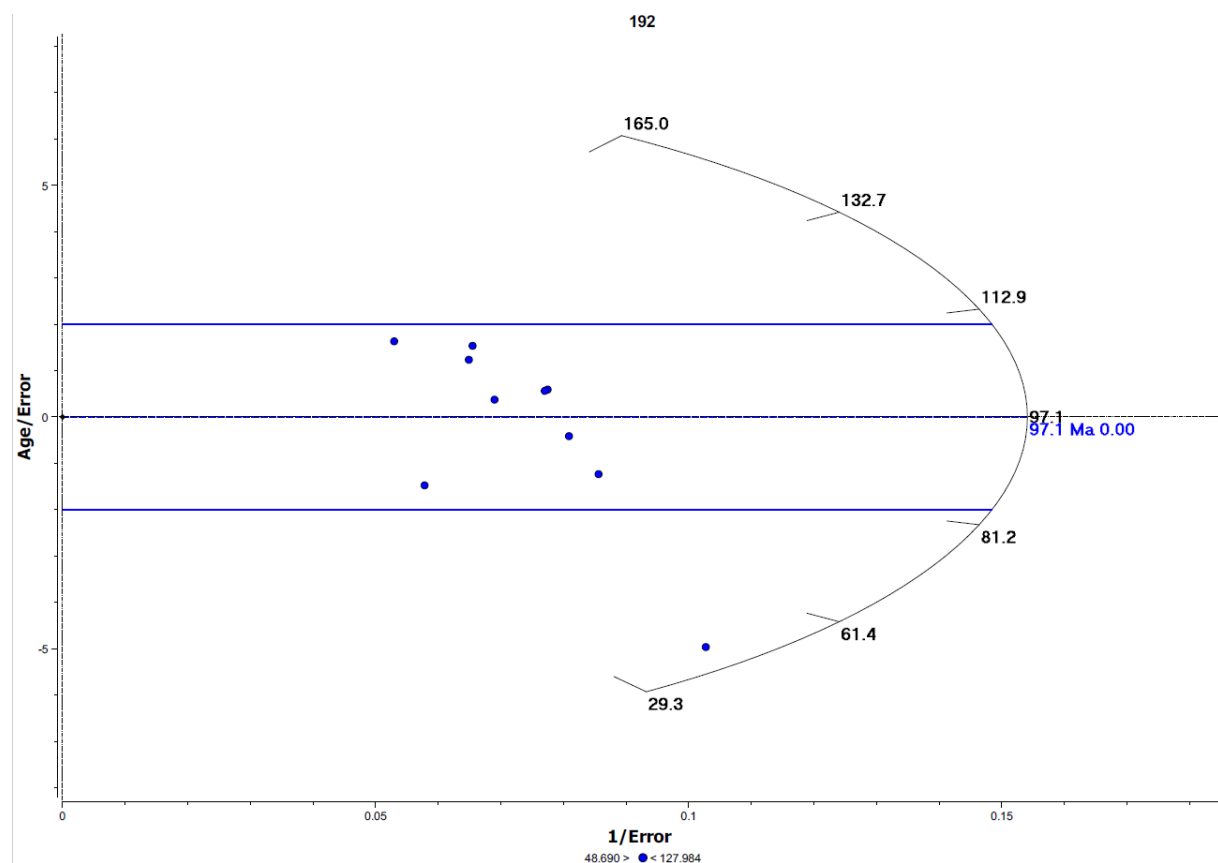


**Figure S.18.** Radial plot for sample 124, constructed using QTQt (Gallagher, 2012).

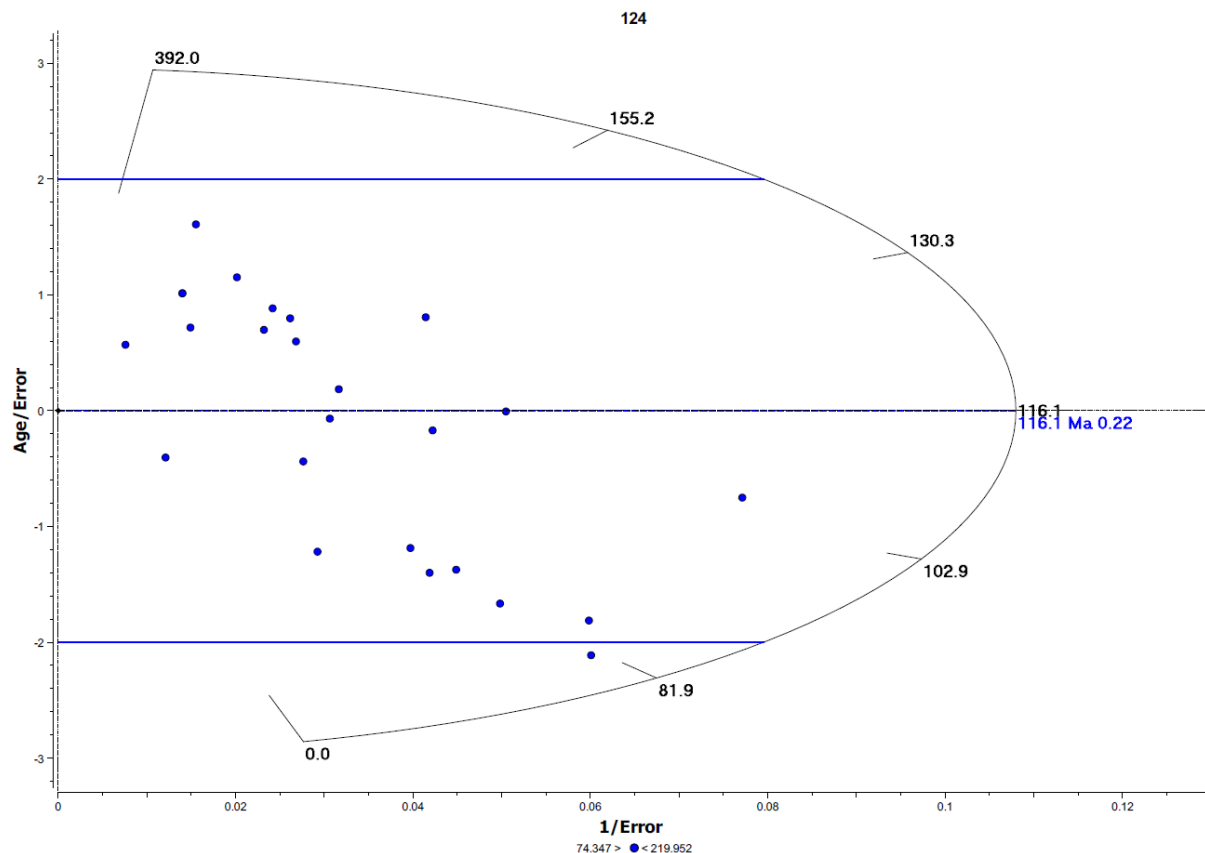


**Figure S.19.** Radial plot for sample 134, constructed using QTQt (Gallagher, 2012).

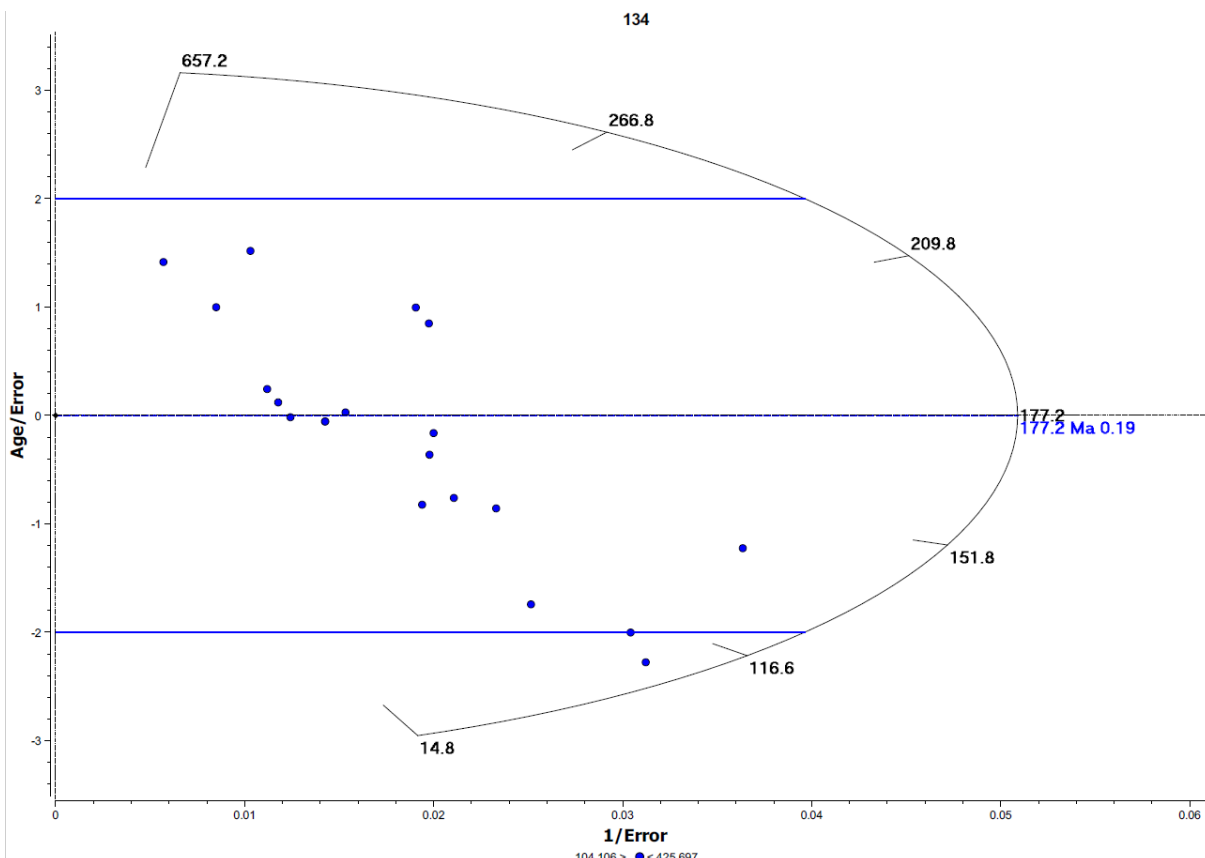
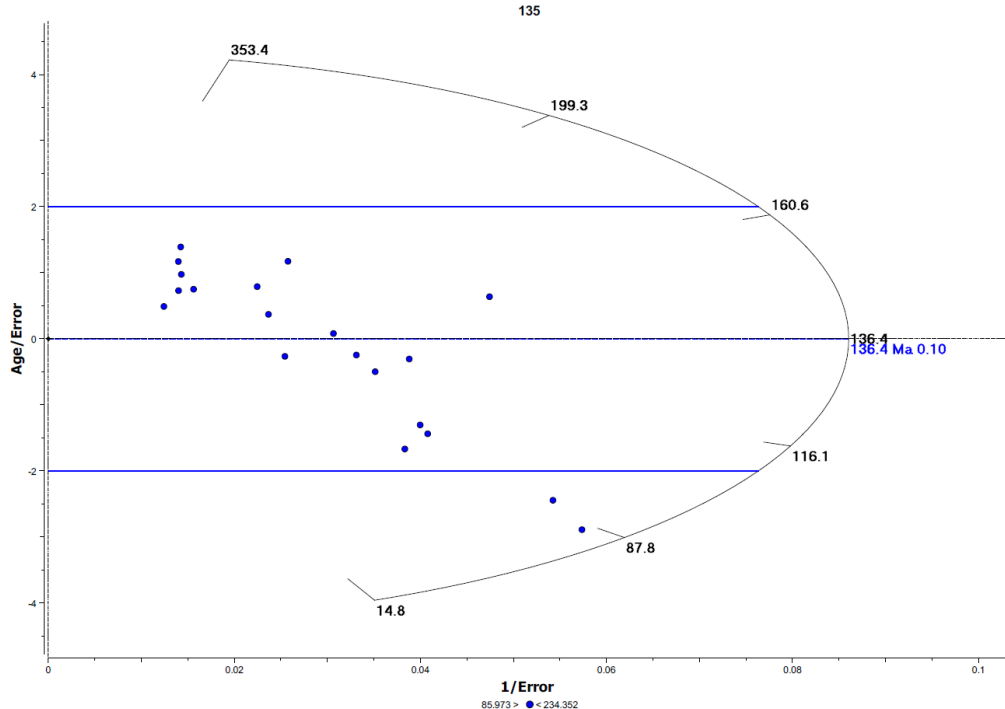


**Figure S.20.** Radial plot for sample 135, constructed using QTQt (Gallagher, 2012).



## S2: Length data

Here we make available the raw data for sub-horizontal confined apatite fission-tracks (length and angle with c-axis) and supporting graphs. Measurements were done using TrackFlow (Van Ranst et al., 2020) using a Nikon Eclipse Ni-E microscope equipped with a DS-Ri2 camera and set to a magnification of 1000x.

**Figure S.21.** Raw track lengths (L) in  $\mu\text{m}$  and angle with c-axis (A) for sample 171.

ID	L	A	ID	L	A	ID	L	A
1	13.6	57.0	35	10.7	60.0	69	11.9	24.0
2	9.4	75.0	36	14.0	37.0	70	6.1	60.0
3	12.4	73.0	37	11.0	54.0	71	11.3	64.0
4	13.6	53.0	38	8.1	76.0	72	10.1	84.0
5	13.8	78.0	39	12.9	69.0	73	9.2	66.0
6	13.2	25.0	40	10.6	68.0	74	10.6	64.0
7	10.7	53.0	41	9.4	80.0	75	8.5	78.0
8	10.7	79.0	42	10.8	27.0	76	12.6	44.0
9	9.9	74.0	43	5.2	84.0	77	11.4	87.0
10	10.1	74.0	44	11.8	63.0	78	12.7	64.0
11	10.0	62.0	45	9.6	24.0	79	12.2	89.0
12	12.4	31.0	46	11.5	36.0	80	10.2	79.0
13	11.6	27.0	47	11.0	60.0	81	9.6	68.0
14	13.0	21.0	48	8.6	36.0	82	13.9	32.0
15	12.7	34.0	49	14.5	41.0	83	10.9	67.0
16	13.1	50.0	50	14.3	63.0	84	8.8	50.0
17	10.6	79.0	51	12.1	72.0	85	13.8	1.0
18	12.0	48.0	52	11.5	58.0	86	12.1	47.0
19	8.8	62.0	53	12.2	17.0	87	12.6	61.0
20	11.6	53.0	54	11.4	75.0	88	12.9	68.0
21	9.8	69.0	55	10.9	50.0	89	9.0	34.0
22	12.1	54.0	56	10.0	56.0	90	8.4	63.0
23	14.0	42.0	57	13.6	80.0	91	13.9	49.0
24	15.1	70.0	58	9.6	34.0	92	12.3	78.0
25	11.4	55.0	59	16.8	48.0	93	12.7	48.0
26	13.8	2.0	60	13.5	24.0	94	12.4	77.0
27	13.4	22.0	61	8.5	84.0	95	16.2	68.0
28	11.2	87.0	62	15.0	50.0	96	9.9	44.0
29	11.6	87.0	63	13.1	37.0	97	13.8	53.0
30	12.6	7.0	64	13.7	29.0	98	12.1	33.0
31	9.0	29.0	65	9.0	62.0	99	11.1	66.0
32	11.6	50.0	66	11.9	86.0	100	10.2	52.0
33	11.3	72.0	67	12.4	84.0			
34	11.1	49.0	68	13.9	55.0			

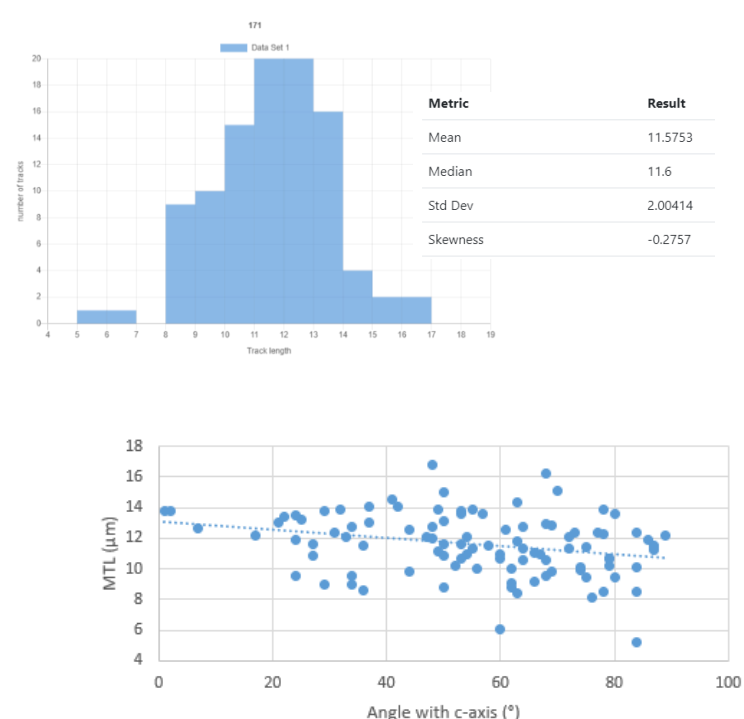


**Figure S.22.** Raw track lengths (L) in  $\mu\text{m}$  and angle with c-axis (A) for sample 175.

ID	L	A	ID	L	A	ID	L	A
1	9.6	70	35	14.4	73	69	10.8	78
2	14.7	69	36	9.7	29	70	14.1	21
3	12.7	56	37	12.7	88	71	11.4	57
4	9.4	2	38	14.0	60	72	9.3	19
5	10.0	21	39	13.3	74	73	12.1	62
6	12.7	47	40	12.8	77	74	9.7	35
7	13.3	24	41	13.2	24	75	11.2	40
8	13.4	46	42	11.9	70	76	13.9	72
9	8.7	39	43	8.5	58	77	10.4	42
10	13.1	59	44	10.3	73	78	10.3	28
11	14.6	48	45	9.0	71	79	12.9	26
12	13.1	61	46	9.0	71	80	14.5	80
13	14.6	76	47	12.1	57	81	9.5	35
14	12.4	73	48	11.7	34	82	8.5	81
15	13.6	49	49	13.7	30	83	14.8	61
16	11.6	53	50	10.9	80	84	13.3	67
17	13.4	30	51	14.2	62	85	9.1	41
18	9.3	55	52	9.3	73	86	10.4	24
19	14.3	82	53	13.2	38	87	12.5	36
20	13.1	57	54	10.8	36	88	14.0	71
21	13.0	49	55	10.8	44	89	11.1	60
22	13.4	22	56	11.4	68	90	12.8	39
23	12.6	68	57	13.4	57	91	12.1	69
24	11.5	36	58	13.7	28	92	11.9	13
25	13.0	87	59	12.9	30	93	13.6	63
26	12.5	77	60	11.4	45	94	12.4	59
27	10.9	39	61	12.7	53	95	11.8	20
28	14.3	58	62	8.0	5	96	12.8	3
29	9.7	61	63	8.5	22	97	11.9	14
30	13.3	48	64	12.0	73	98	11.3	43
31	11.5	73	65	13.4	54	99	8.7	27
32	10.3	61	66	12.0	42	100	11.6	66
33	13.3	35	67	11.9	78			
34	12.0	68	68	9.8	30			

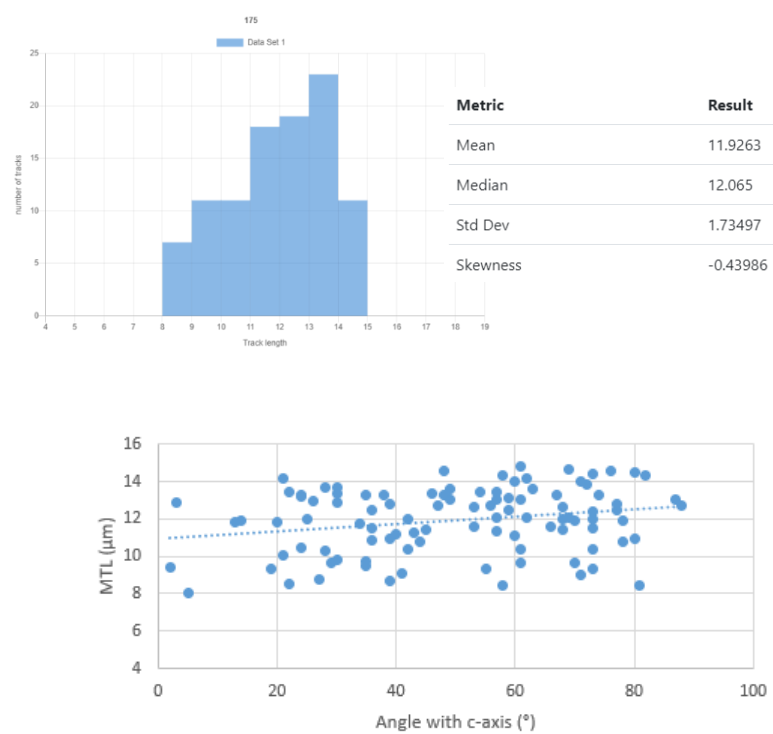


**Figure S.23.** Raw track lengths (L) in  $\mu\text{m}$  and angle with c-axis (A) for sample 176.

ID	L	A	ID	L	A	ID	L	A
1	11.3	53	35	13.2	75	69	12.5	84
2	14.8	54	36	12.2	64	70	12.5	77
3	10.9	55	37	13.4	48	71	11.0	55
4	14.1	70	38	11.9	59	72	13.3	41
5	10.6	46	39	8.1	53	73	11.9	46
6	10.7	37	40	11.7	79	74	8.4	62
7	12.8	79	41	10.8	85	75	9.5	49
8	8.2	33	42	12.0	88	76	13.2	40
9	11.3	25	43	13.0	21	77	14.5	70
10	14.4	70	44	12.2	60	78	13.4	78
11	11.7	58	45	12.2	69	79	9.7	45
12	10.9	88	46	13.8	26	80	10.5	75
13	11.5	76	47	12.8	55	81	12.2	42
14	14.4	19	48	13.2	82	82	12.5	74
15	11.6	51	49	12.6	55	83	10.7	60
16	13.4	24	50	13.4	50	84	15.1	56
17	10.3	66	51	10.5	90	85	11.4	74
18	13.2	32	52	15.1	40	86	11.1	62
19	8.6	77	53	12.6	52	87	12.1	75
20	11.4	66	54	10.7	86	88	10.6	44
21	9.2	46	55	12.7	60	89	12.1	70
22	10.5	78	56	13.5	62	90	13.2	83
23	12.6	85	57	12.7	70	91	10.8	81
24	12.9	72	58	11.6	58	92	13.6	60
25	12.2	76	59	9.4	73	93	13.4	20
26	11.9	59	60	10.3	56	94	11.3	51
27	10.1	19	61	12.0	54	95	11.0	83
28	10.7	34	62	9.0	46	96	12.3	53
29	9.8	76	63	10.2	87	97	13.2	54
30	13.6	50	64	13.6	46	98	12.2	66
31	10.5	84	65	9.7	51	99	14.5	46
32	8.1	38	66	10.3	50	100	14.0	41
33	14.0	81	67	14.5	60			
34	11.9	72	68	9.8	78			

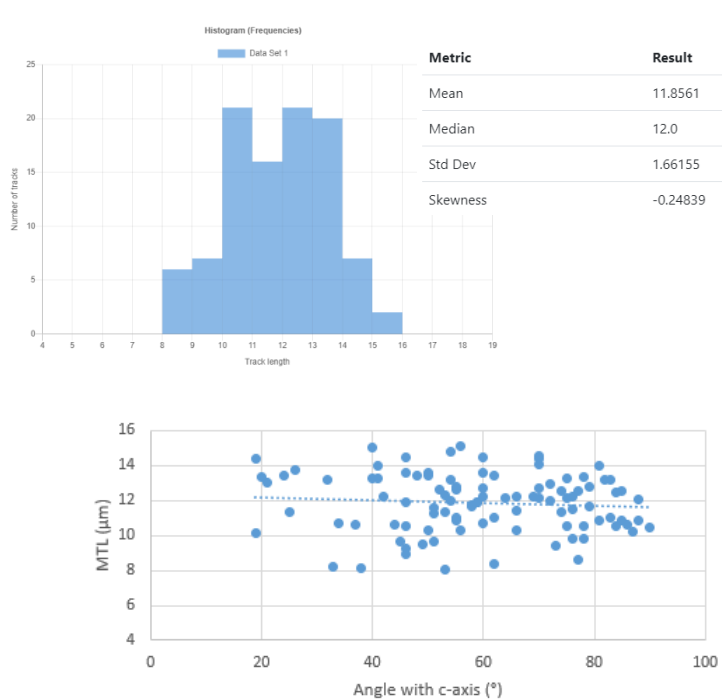


**Figure S.24.** Raw track lengths (L) in  $\mu\text{m}$  and angle with c-axis (A) for sample 180.

ID	L	A	ID	L	A	ID	L	A
1	9.1	41.00	35	8.8	73	69	13.5	73
2	11.2	50.00	36	9.2	71	70	12.8	39
3	12.6	67.00	37	11.0	53	71	13.2	30
4	13.4	69.00	38	10.6	13	72	13.8	30
5	9.2	56.00	39	10.0	66	73	11.0	74
6	9.0	43.00	40	10.5	61	74	13.1	50
7	12.2	30.00	41	13.9	77	75	15.5	34
8	11.2	55.00	42	13.6	29	76	11.8	73
9	9.2	45.00	43	13.5	76	77	11.8	67
10	10.7	51.00	44	12.6	11	78	14.3	74
11	10.8	66.00	45	14.0	74	79	13.9	33
12	10.4	71.00	46	12.1	58	80	12.8	25
13	7.9	82.00	47	12.0	50	81	10.0	68
14	9.7	28.00	48	13.9	23	82	11.1	64
15	9.3	67.00	49	10.8	87	83	12.0	53
16	8.4	70.00	50	10.5	49	84	11.7	39
17	12.8	50.00	51	12.9	55	85	12.0	40
18	12.9	58.00	52	11.8	85	86	12.9	67
19	12.5	56.00	53	9.5	49	87	12.9	65
20	12.1	36.00	54	12.7	86	88	10.1	60
21	11.3	42.00	55	13.7	29	89	12.9	86
22	12.0	45.00	56	10.9	69	90	5.6	77
23	9.8	86.00	57	10.2	58	91	13.8	67
24	11.2	68.00	58	14.2	43	92	12.4	57
25	13.9	11.00	59	12.3	65	93	9.1	84
26	12.3	75.00	60	12.3	86	94	13.4	56
27	12.4	47.00	61	12.8	1	95	11.9	35
28	12.8	42.00	62	12.6	57	96	12.1	34
29	12.1	62.00	63	13.9	32	97	14.4	25
30	11.6	82.00	64	12.4	79	98	10.2	62
31	11.4	40.00	65	11.5	63	99	12.3	48
32	8.7	60.00	66	9.9	49	100	8.7	68
33	12.1	65.00	67	13.9	72			
34	13.2	53.51	68	10.9	27			

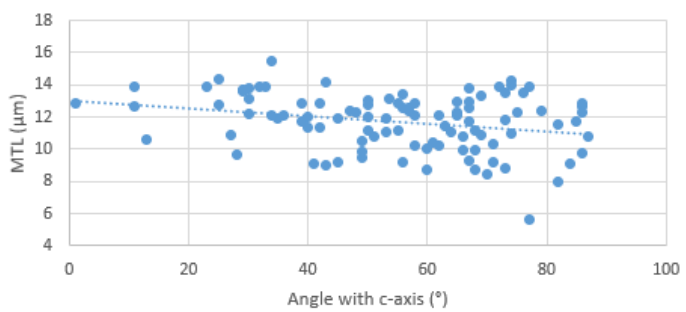
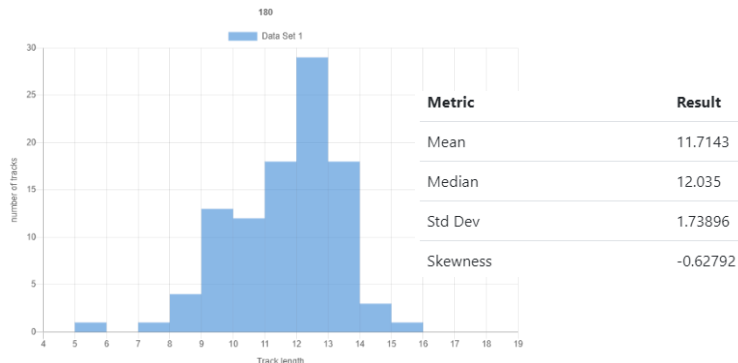


**Figure S.25.** Raw track lengths (L) in  $\mu\text{m}$  and angle with c-axis (A) for sample 182.

ID	L	A	ID	L	A	ID	L	A
1	11.2	46	35	11.5	84	69	12.3	60
2	12.0	12	36	13.5	60	70	14.4	40
3	12.5	44	37	12.3	82	71	13.5	31
4	12.2	52	38	12.5	80	72	12.3	15
5	10.7	58	39	13.9	74	73	13.9	43
6	13.3	43	40	9.7	70	74	10.8	56
7	14.3	62	41	14.1	84	75	12.9	60
8	11.7	85	42	10.5	80	76	11.5	53
9	12.7	73	43	11.9	62	77	12.2	59
10	14.4	30	44	12.9	79	78	12.4	64
11	11.4	50	45	14.1	66	79	7.8	79
12	12.7	76	46	13.7	23	80	7.8	64
13	13.1	56	47	12.9	47	81	13.2	50
14	13.9	47	48	10.4	50	82	15.7	34
15	12.2	78	49	14.2	60	83	12.5	62
16	13.4	27	50	12.2	77	84	13.3	41
17	12.4	50	51	10.9	32	85	12.2	64
18	12.6	39	52	12.8	56	86	12.8	43
19	12.5	54	53	11.6	54	87	12.7	41
20	14.0	49	54	12.7	68	88	14.8	39
21	11.9	44	55	13.2	50	89	12.7	65
22	10.3	63	56	13.6	38	90	10.1	71
23	11.8	40	57	9.2	68	91	7.7	76
24	11.2	57	58	8.3	80	92	14.6	54
25	13.3	36	59	12.2	69	93	13.1	66
26	11.9	88	60	12.8	70	94	12.9	48
27	13.7	60	61	12.9	35	95	12.2	55
28	11.3	70	62	14.8	68	96	13.0	45
29	12.7	19	63	14.6	36	97	12.2	39
30	11.9	75	64	11.4	68	98	14.3	46
31	13.6	77	65	9.5	39	99	13.1	27
32	13.6	45	66	15.7	36	100	13.1	44
33	13.6	81	67	12.0	71			
34	13.0	67	68	12.4	67			

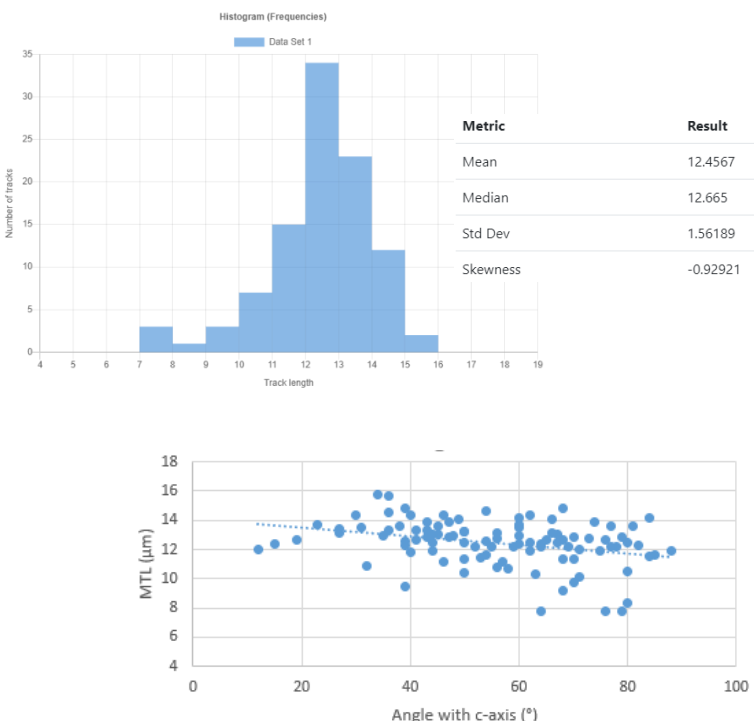


**Figure S.26.** Raw track lengths (L) in  $\mu\text{m}$  and angle with c-axis (A) for sample 164.

ID	L	A
1	11.1	54
2	10.3	71
3	12.3	75
4	11.0	73
5	8.0	54
6	9.2	89
7	6.7	51
8	10.2	45
9	13.8	83
10	13.3	60
11	12.7	29
12	11.8	86
13	13.3	52
14	8.8	68
15	13.7	73
16	12.2	77
17	12.8	61
18	8.8	71
19	14.7	64
20	13.5	41
21	14.2	33

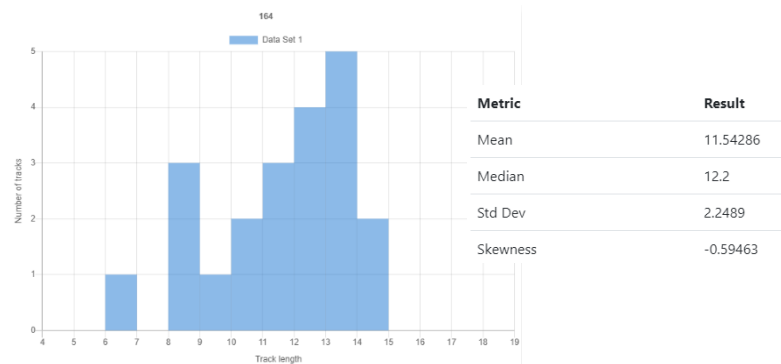


**Figure S.27.** Raw track lengths (L) in  $\mu\text{m}$  and angle with c-axis (A) for sample 168.

ID	L	A
1	12.5	63
2	14.5	66
3	13.5	17
4	12.1	47
5	13.3	86
6	14.2	48
7	13.5	74
8	13.1	53
9	13.2	45
10	14.5	58
11	12.7	63
12	13.7	51
13	12.5	71
14	12.0	8
15	12.6	16
16	12.9	37
17	10.1	52
18	12.5	45
19	11.9	35
20	13.5	1
21	11.5	64
22	15.0	37
23	13.0	16
24	13.9	36
25	11.0	34
26	14.5	45
27	11.6	20

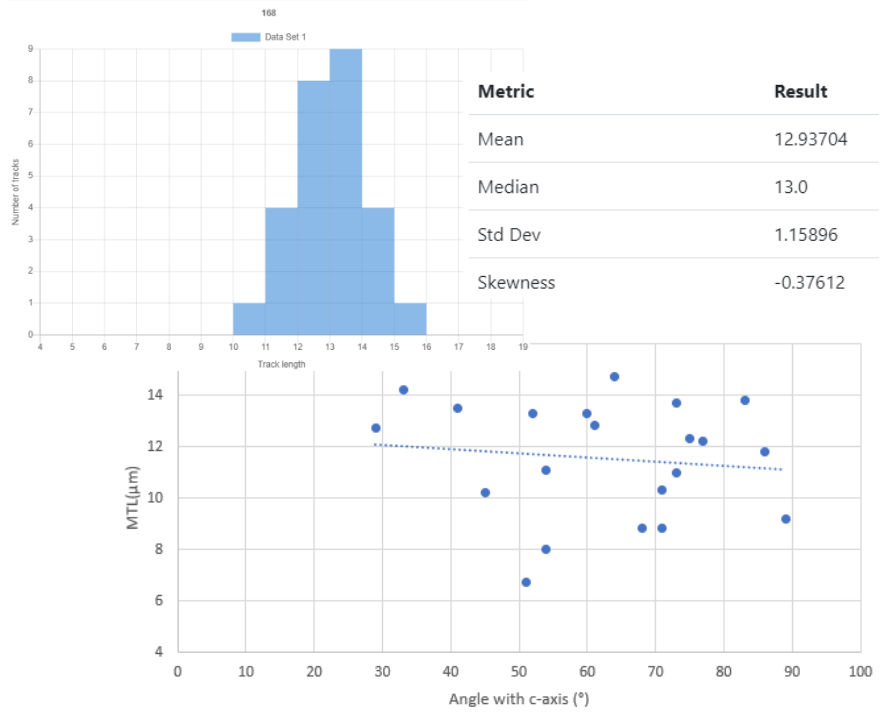


**Figure S.28.** Raw track lengths (L) in  $\mu\text{m}$  and angle with c-axis (A) for sample 170.

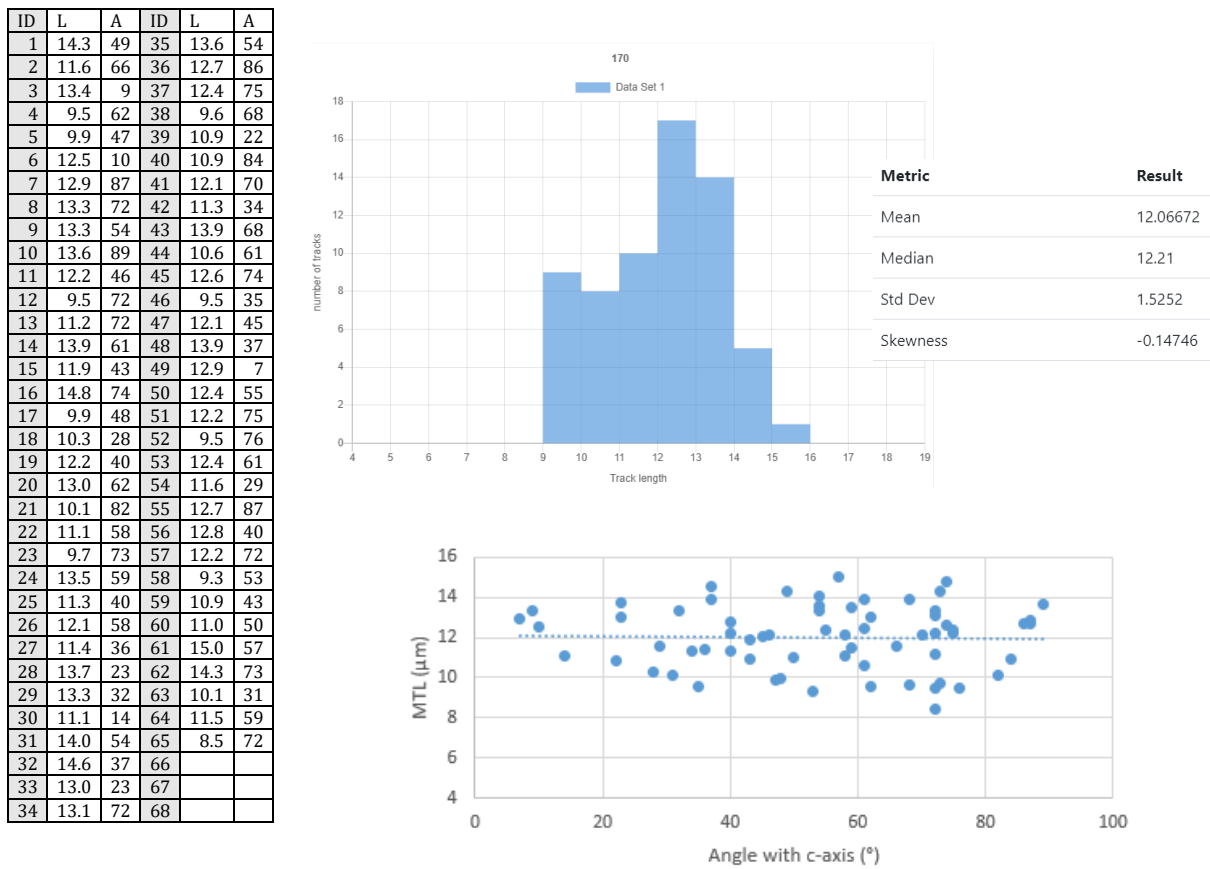


**Figure S.29.** Raw track lengths (L) in  $\mu\text{m}$  and angle with c-axis (A) for sample 501.

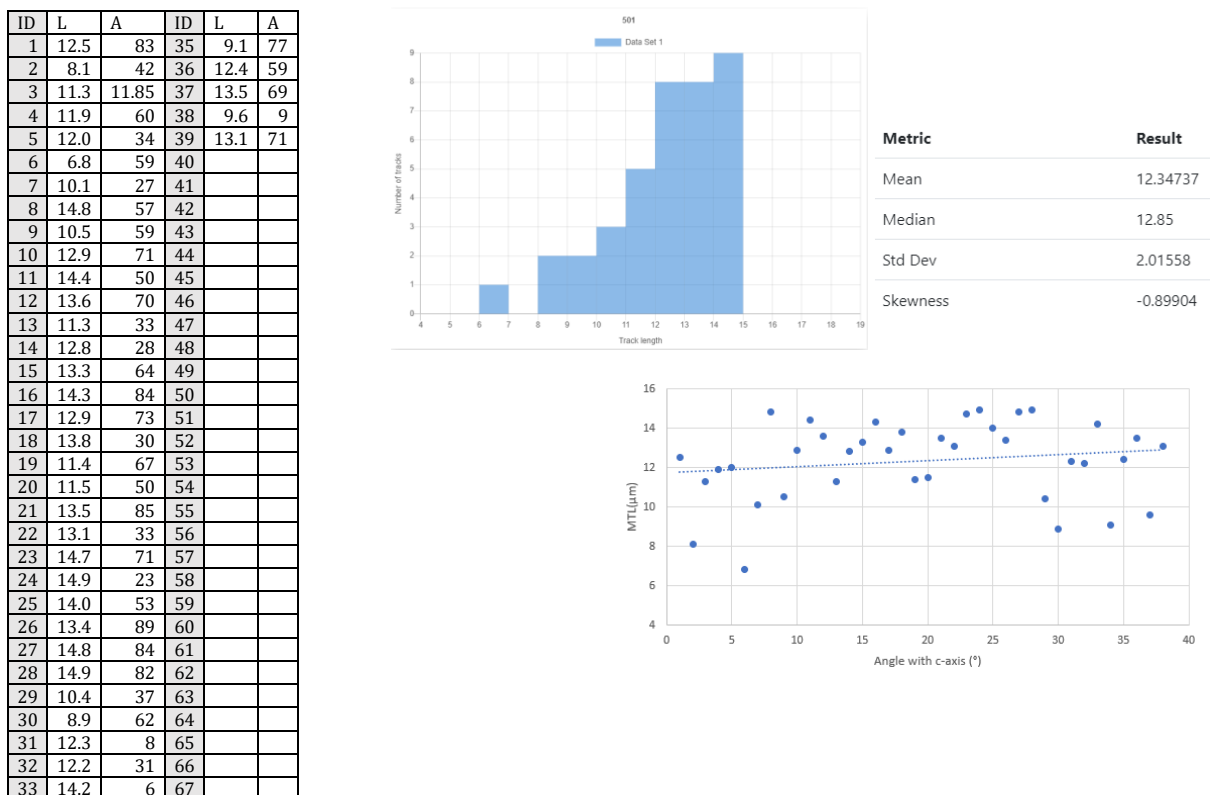


**Figure S.30.** Raw track lengths (L) in  $\mu\text{m}$  and angle with c-axis (A) for sample 502.

ID	L	A	ID	L	A	ID	L	A
1	14.2	45	35	12.4	26	69	10.7	80
2	9.9	75	36	9.1	65	70	10.1	37
3	7.9	48	37	14.0	45	71	12.2	41
4	13.0	54	38	13.7	65	72	12.6	47
5	10.7	56	39	15.1	54	73	11.8	77
6	13.5	76	40	11.8	42	74	13.1	48
7	10.6	65	41	11.6	45	75	12.3	45
8	9.2	75	42	11.9	48	76	13.7	9
9	9.9	57	43	13.1	21	77	13.5	23
10	10.5	73	44	13.2	31	78	12.2	12
11	13.7	58	45	13.5	88	79	12.5	31
12	12.3	54	46	11.3	49	80	9.7	43
13	11.3	78	47	12.8	89	81	11.8	35
14	11.4	61	48	11.4	66	82	12.0	36
15	11.9	77	49	10.8	80	83	12.6	54
16	11.5	64	50	9.6	48	84	11.7	52
17	9.6	49	51	13.3	88	85	11.8	74
18	13.3	50	52	12.1	73	86	13.6	54
19	10.4	73	53	10.9	57	87	12.4	68
20	10.0	62	54	12.0	52	88	12.8	42
21	13.8	56	55	12.5	88	89	11.6	71
22	12.8	71	56	11.6	86	90	14.1	41
23	11.0	59	57	10.4	42	91	12.5	72
24	12.5	45	58	11.0	85	92	11.5	70
25	11.0	79	59	13.3	69	93	12.3	80
26	11.0	76	60	12.8	62	94	11.4	80
27	10.1	52	61	14.4	48	95	11.5	69
28	14.8	73	62	11.9	85	96	11.5	40
29	12.1	61	63	14.4	44	97	14.5	53
30	12.0	56	64	7.7	74	98	11.3	30
31	13.0	51	65	8.9	28	99	12.8	50
32	7.6	60	66	13.1	49	100	9.0	73
33	10.2	31	67	11.6	47			
34	13.2	19	68	12.3	34			

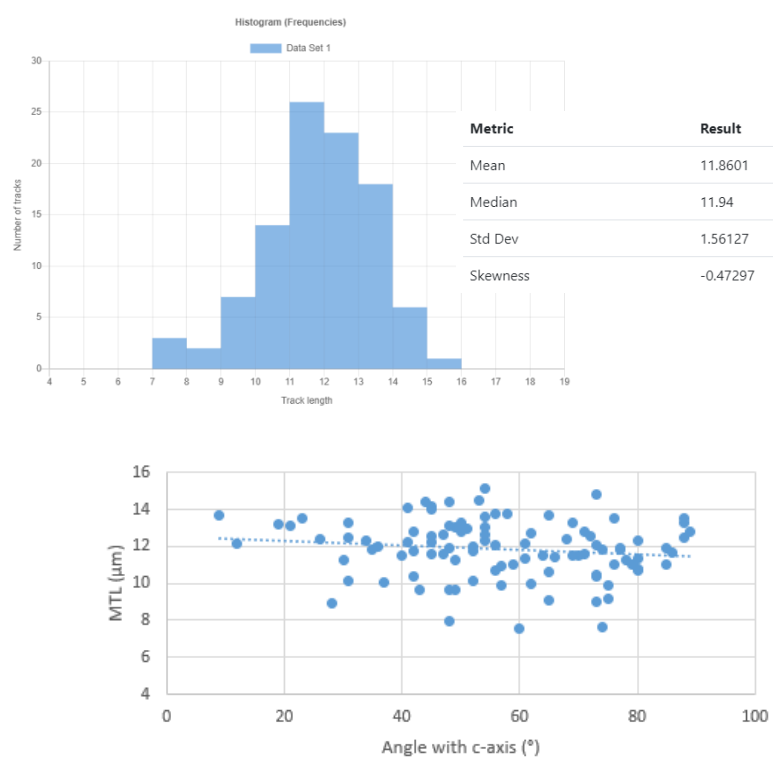
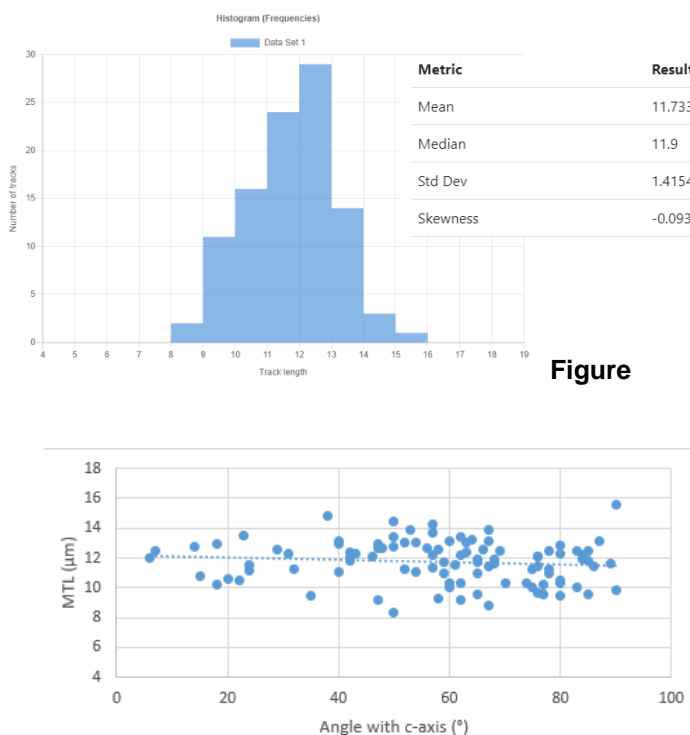


**Figure S.31.** Raw track lengths (L) in  $\mu\text{m}$  and angle with c-axis (A) for sample 505.

ID	L	A	ID	L	A	ID	L	A
1	10.1	77	35	12.6	55	69	11.2	32
2	10.0	81	36	8.7	41	70	11.0	42
3	12.0	61	37	9.1	79	71	10.6	66
4	12.1	47	38	11.4	76	72	11.1	61
5	9.9	66	39	12.4	61	73	9.6	51
6	11.4	85	40	12.4	70	74	9.6	78
7	10.0	86	41	12.5	53	75	11.1	53
8	12.0	90	42	12.6	80	76	12.0	59
9	9.1	78	43	12.4	47	77	9.2	52
10	7.6	39	44	8.3	35	78	8.1	10
11	11.8	62	45	13.1	63	79	11.9	66
12	8.3	58	46	8.1	75	80	10.8	34
13	9.0	53	47	9.3	73	81	10.7	82
14	10.7	49	48	10.0	79	82	9.5	42
15	11.7	39	49	12.1	17	83	6.9	35
16	11.3	70	50	11.8	69	84	10.9	19
17	10.7	61	51	12.6	55	85	11.7	51
18	12.8	78	52	9.5	45	86	11.7	63
19	13.0	52	53	10.9	43	87	10.5	23
20	12.5	54	54	7.7	45	88	8.0	80
21	13.2	44	55	9.2	66	89	10.3	36
22	9.3	71	56	9.1	71	90	11.8	58
23	12.3	74	57	11.5	75	91	10.1	79
24	10.1	70	58	8.7	41	92	9.9	59
25	9.2	60	59	10.1	55	93	7.5	29
26	11.4	63	60	8.0	33	94	12.2	75
27	11.7	78	61	12.4	43	95	9.3	30
28	10.7	42	62	10.0	38	96	8.5	75
29	11.1	74	63	11.2	83	97	12.0	71
30	10.2	79	64	12.3	49	98	13.9	76
31	9.2	73	65	10.4	49	99	12.1	78
32	11.9	33	66	12.5	51	100	10.5	33
33	7.0	57	67	11.2	59			
34	9.1	68	68	10.5	35			



**Figure**

**S.32.** Raw track lengths (L) in  $\mu\text{m}$  and angle with c-axis (A) for sample 506.

ID	L	A	ID	L	A	ID	L	A
1	13.7	17	35	12.2	68	69	13.0	74
2	9.8	62	36	12.8	29	70	10.4	82
3	9.1	60	37	11.6	71	71	10.3	33
4	7.3	38	38	14.1	80	72	14.0	29
5	11.6	48	39	11.6	60	73	11.2	55
6	8.4	59	40	9.6	63	74	10.6	46
7	11.5	82	41	11.4	49	75	13.4	46
8	9.7	49	42	10.4	39	76	13.3	40
9	13.9	28	43	15.8	73	77	11.1	21
10	11.9	39	44	10.8	70	78	12.7	69
11	10.9	49	45	12.3	63	79	13.1	28
12	13.4	39	46	12.7	31	80	14.0	62
13	10.7	26	47	10.1	60	81	11.7	78
14	14.8	36	48	12.2	78	82	12.2	70
15	12.0	19	49	14.0	30	83	11.7	75
16	13.8	69	50	12.9	25	84	12.9	58
17	11.8	59	51	13.8	34	85	9.0	58
18	11.0	83	52	14.0	49	86	14.3	19
19	13.7	45	53	11.6	35	87	12.4	74
20	14.3	41	54	13.3	20	88	12.1	74
21	12.1	66	55	14.4	50	89	12.7	76
22	12.3	58	56	11.5	83	90	9.7	38
23	10.8	2	57	13.0	60	91	12.6	57
24	13.7	75	58	12.3	54	92	11.4	60
25	10.8	73	59	12.5	53	93	13.2	51
26	12.1	70	60	11.6	40	94	10.1	67
27	14.8	37	61	14.2	74	95	13.5	72
28	12.4	66	62	12.1	57	96	13.4	43
29	14.4	35	63	12.5	69	97	13.9	83
30	14.6	74	64	11.2	57	98	13.3	23
31	12.4	77	65	14.0	26	99	14.4	15
32	14.0	23	66	12.6	69	100	12.7	65
33	8.2	50	67	13.1	64			
34	11.6	24	68	11.5	84			

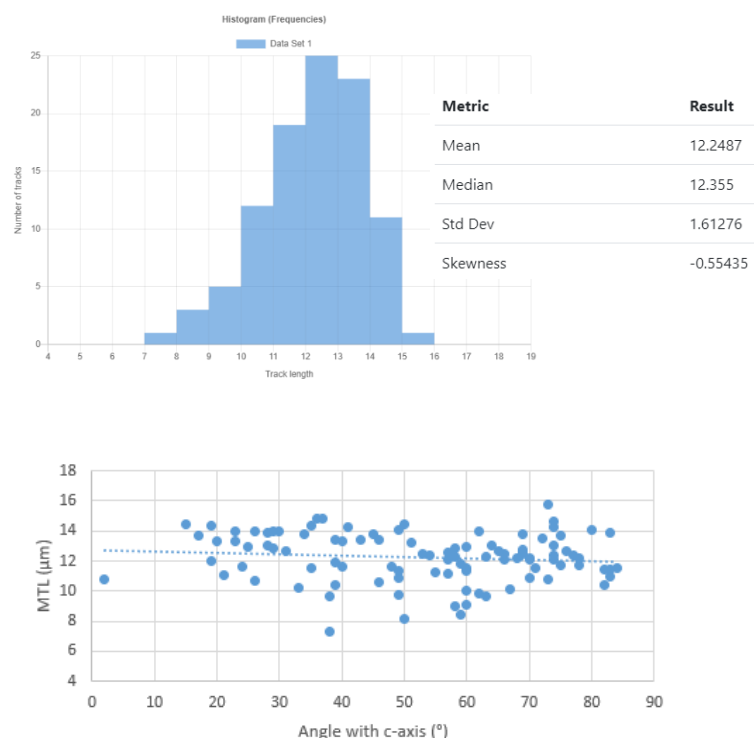


**Figure S.33.** Raw track lengths (L) in  $\mu\text{m}$  and angle with c-axis (A) for sample 510.

ID	L	A	ID	L	A	ID	L	A
1	11.0	64	35	12.4	67	69	8.7	54
2	12.9	51	36	13.2	67	70	13.2	78
3	10.2	56	37	10.8	67	71	13.0	53
4	13.5	50	38	16.8	74	72	12.3	27
5	9.8	56	39	10.1	61	73	14.6	73
6	14.5	45	40	10.5	69	74	15.8	29
7	13.5	56	41	14.5	76	75	11.9	73
8	11.4	41	42	11.2	75	76	14.1	32
9	10.6	37	43	12.5	66	77	11.2	74
10	12.1	39	44	14.4	63	78	13.3	70
11	11.8	51	45	13.6	78	79	10.3	62
12	13.4	49	46	10.9	62	80	10.9	60
13	12.4	53	47	14.2	64	81	10.9	52
14	10.2	83	48	12.5	48	82	13.1	78
15	14.8	55	49	10.4	89	83	10.2	45
16	14.3	75	50	12.2	82	84	12.1	70
17	13.9	52	51	11.2	89	85	13.1	73
18	14.4	48	52	11.7	55	86	13.7	34
19	13.6	36	53	12.4	76	87	13.8	62
20	13.0	74	54	12.9	14	88	12.9	76
21	8.3	71	55	9.8	73	89	11.6	37
22	13.1	73	56	11.5	38	90	11.8	45
23	14.9	53	57	11.4	77	91	11.8	83
24	13.1	85	58	13.3	48	92	10.1	80
25	12.8	71	59	10.9	32	93	12.1	79
26	11.7	72	60	12.6	47	94	12.1	54
27	11.8	82	61	11.4	66	95	14.3	77
28	11.5	64	62	11.6	55	96	12.4	28
29	12.5	63	63	11.1	58	97	13.3	72
30	11.9	75	64	13.4	40	98	13.5	53
31	13.1	82	65	13.2	30	99	12.1	85
32	9.1	44	66	12.0	83	100	14.2	67
33	13.0	59	67	14.3	56			
34	12.3	45	68	11.0	43			

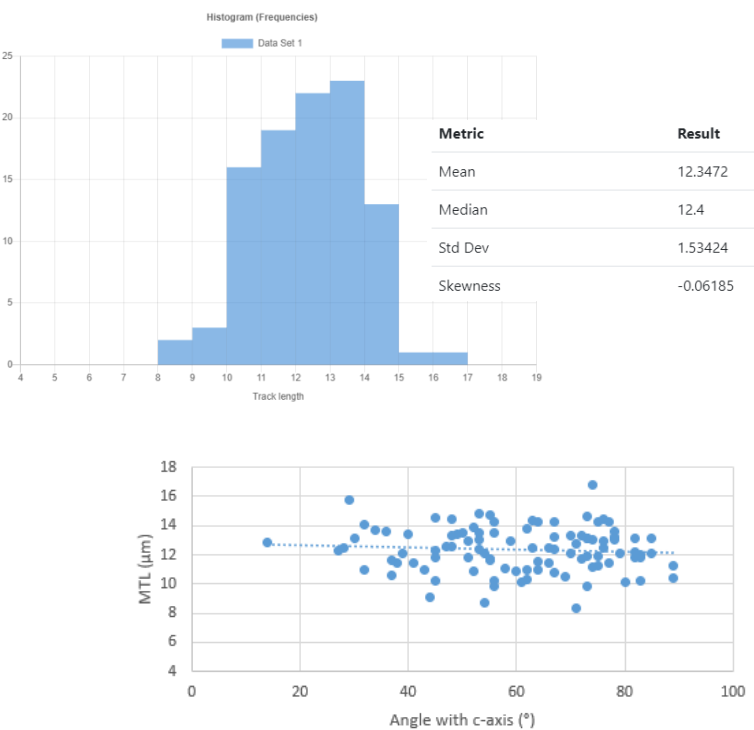


**Figure S.34.** Raw track lengths (L) in  $\mu\text{m}$  and angle with c-axis (A) for sample 512.

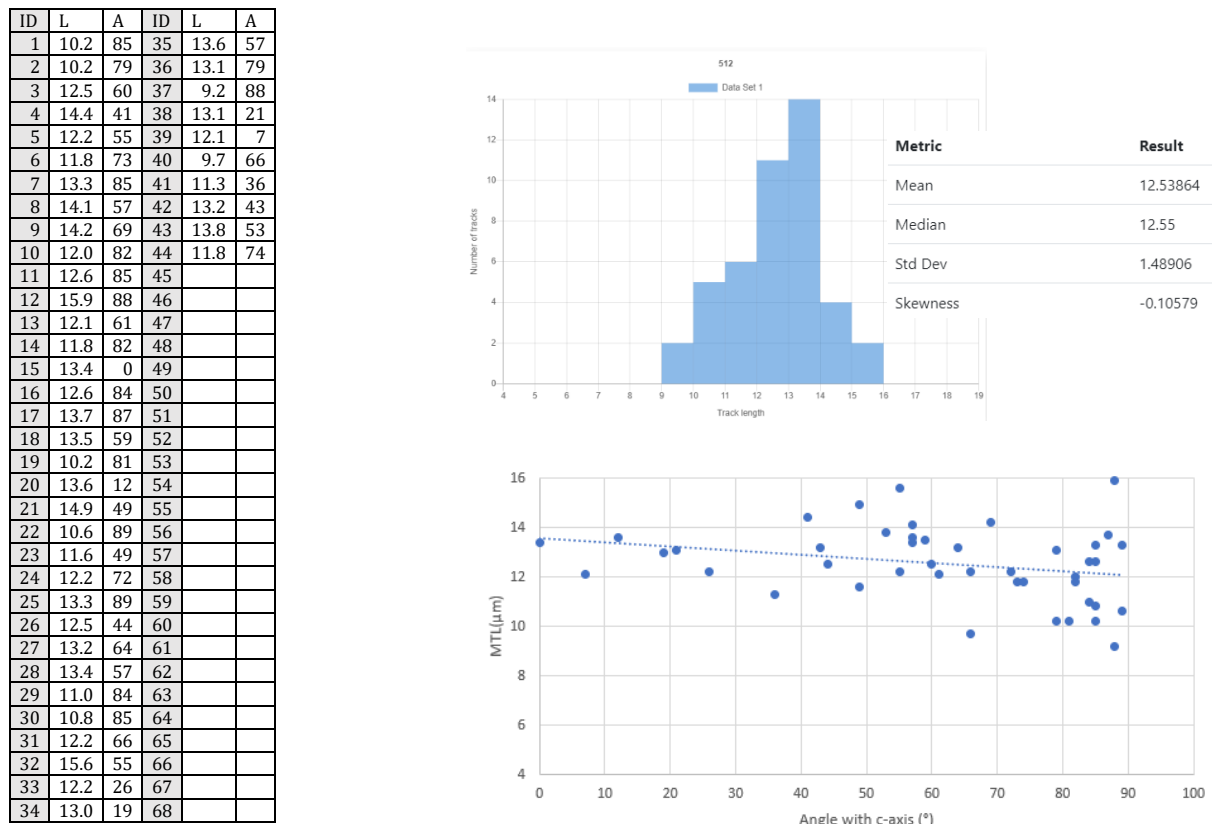


**Figure S.35.** Raw track lengths (L) in  $\mu\text{m}$  and angle with c-axis (A) for sample 515.

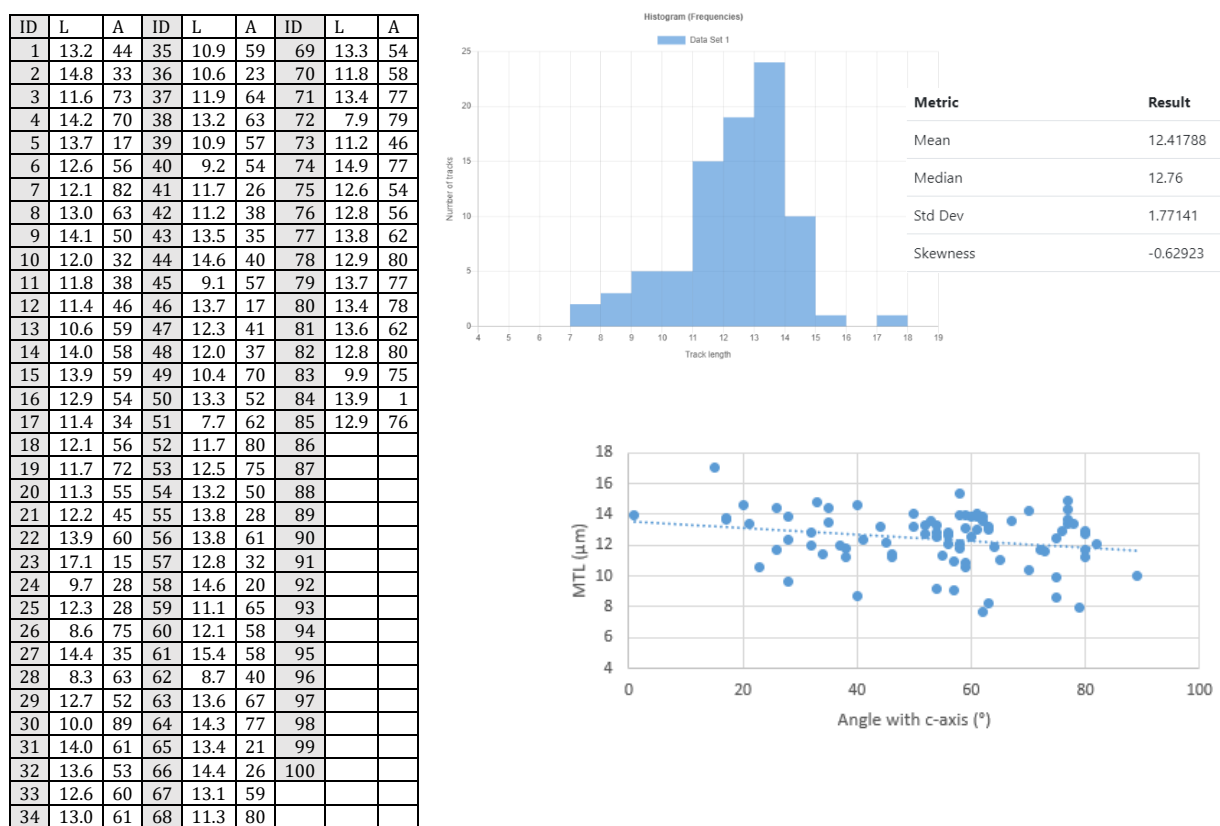


**Figure S.36.** Raw track lengths (L) in  $\mu\text{m}$  and angle with c-axis (A) for sample 516.

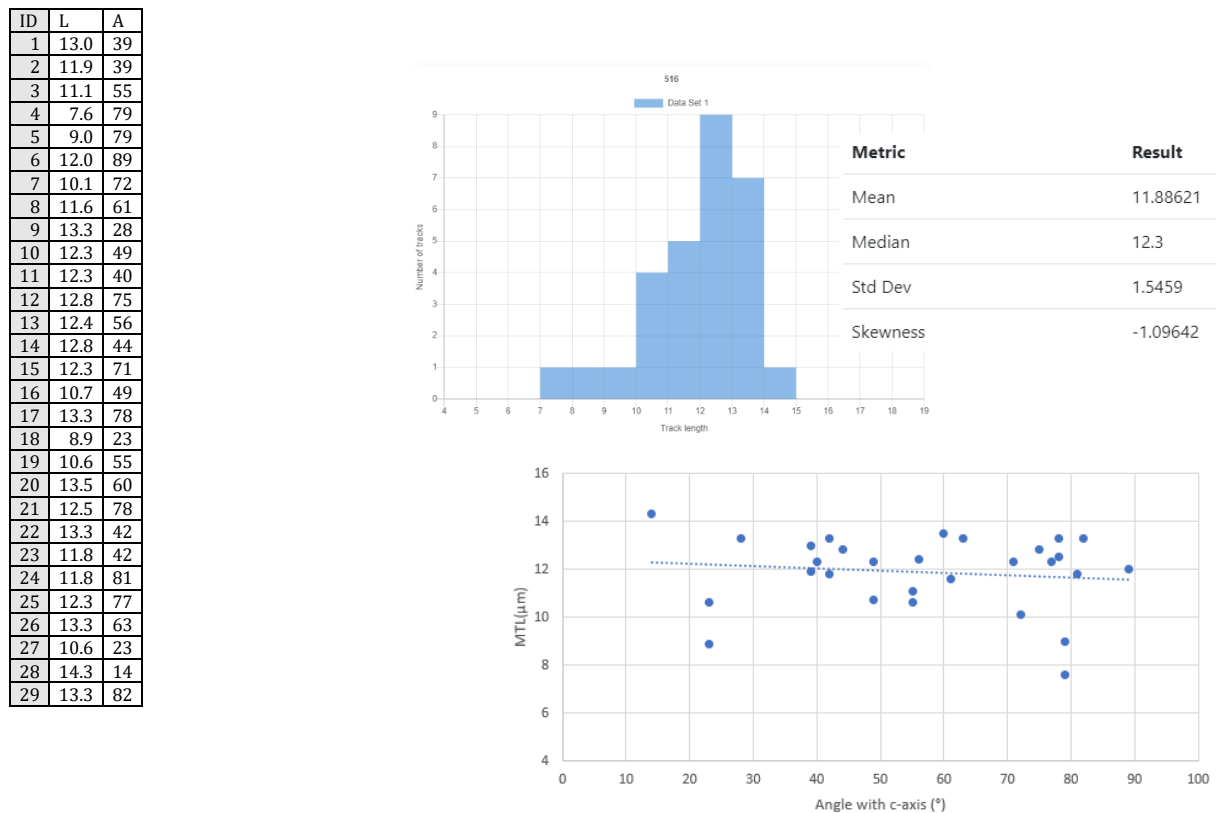


**Figure S.37.** Raw track lengths (L) in  $\mu\text{m}$  and angle with c-axis (A) for sample 192.

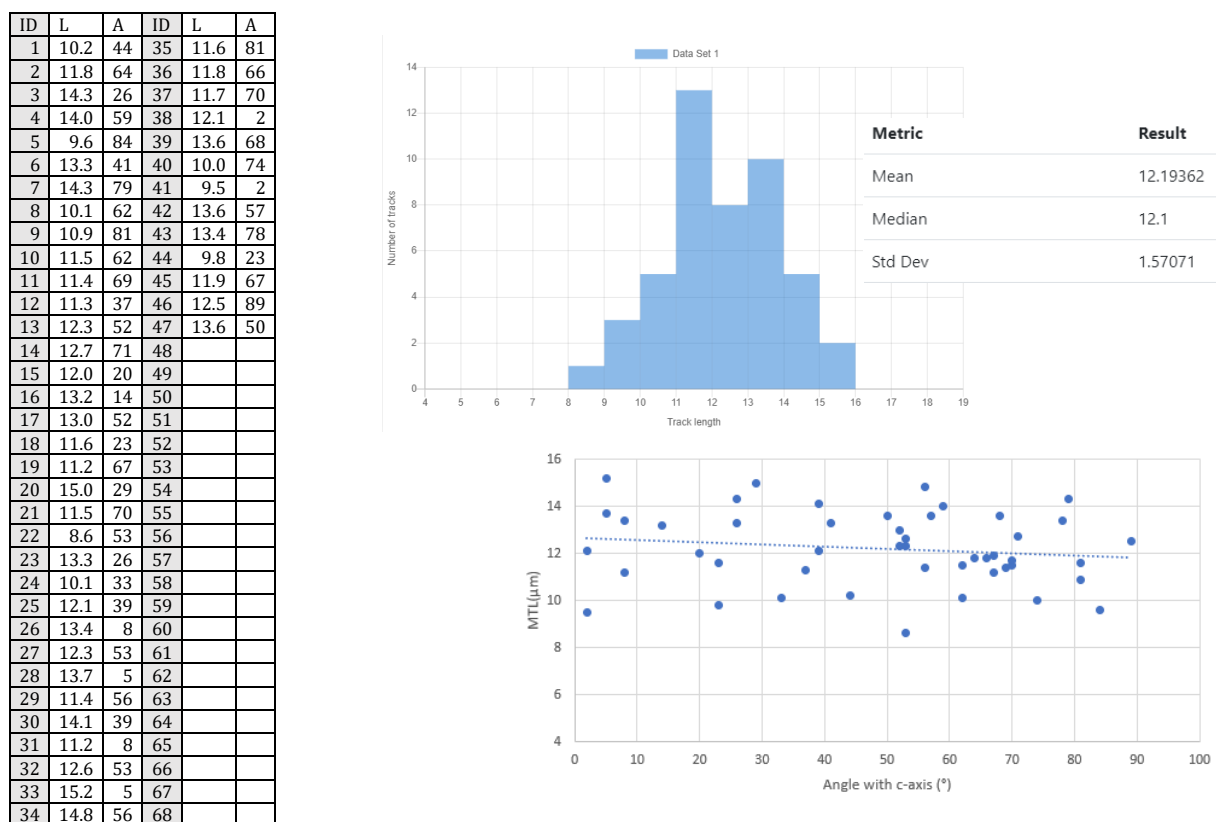


**Figure S.38.** Raw track lengths (L) in  $\mu\text{m}$  and angle with c-axis (A) for sample 124.

ID	L	A	ID	L	A	ID	L	A
1	13.7	51	35	13.2	79	69	12.4	67
2	13.3	49	36	12.3	39	70	14.0	48
3	11.2	18	37	11.3	74	71	13.0	66
4	12.4	41	38	12.7	78	72		
5	10.3	60	39	12.1	50	73		
6	12.4	82	40	13.4	19	74		
7	11.2	70	41	10.2	86	75		
8	11.6	79	42	11.0	45	76		
9	8.3	89	43	12.4	39	77		
10	12.5	47	44	11.9	60	78		
11	12.2	72	45	9.2	50	79		
12	13.8	44	46	10.2	70	80		
13	13.7	73	47	13.7	62	81		
14	14.9	67	48	8.0	78	82		
15	14.7	59	49	11.3	54	83		
16	11.0	84	50	14.6	57	84		
17	12.9	71	51	12.5	33	85		
18	12.6	14	52	12.3	36	86		
19	11.0	25	53	12.2	70	87		
20	13.0	89	54	11.5	37	88		
21	14.1	73	55	11.9	28	89		
22	13.0	77	56	12.2	45	90		
23	12.4	36	57	12.6	81	91		
24	11.0	36	58	11.5	55	92		
25	12.4	39	59	13.7	61	93		
26	8.9	61	60	10.1	22	94		
27	10.7	61	61	13.9	45	95		
28	9.3	72	62	12.7	62	96		
29	11.9	52	63	11.0	22	97		
30	11.2	39	64	11.0	60	98		
31	14.9	61	65	9.4	51	99		
32	10.2	61	66	13.1	31	100		
33	9.4	72	67	12.8	6			
34	13.9	52	68	12.3	70			

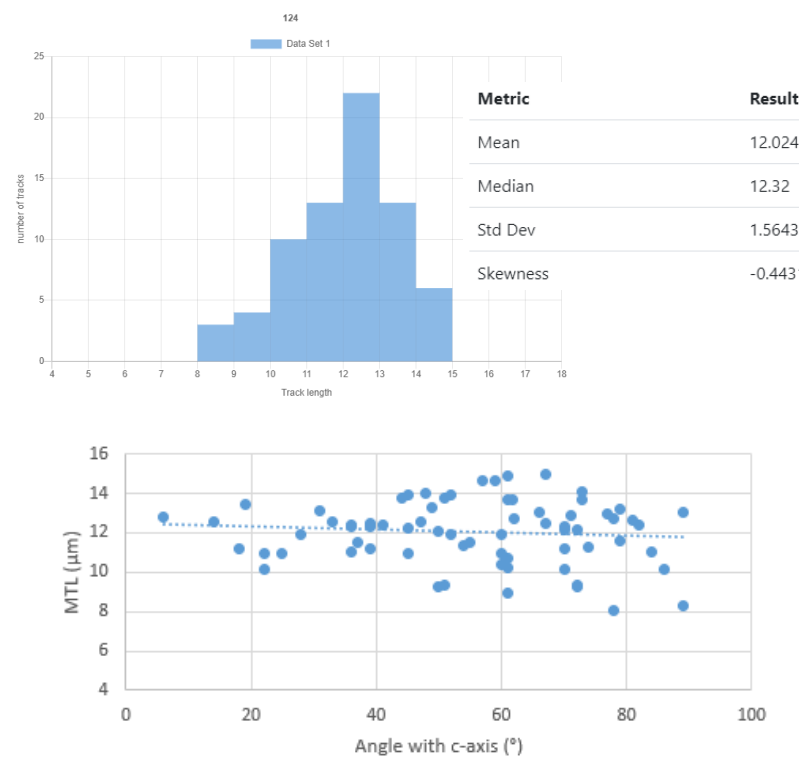


**Figure S.39.** Raw track lengths (L) in  $\mu\text{m}$  and angle with c-axis (A) for sample 134.

ID	L	A
1	11.9	70
2	13.7	41
3	13.5	71
4	13.3	42
5	11.7	73
6	12.8	68
7	13.0	52
8	13.1	69
9	14.2	44
10	10.1	32
11	10.3	63
12	12.2	38
13	11.1	71
14	11.9	78
15	12.8	41
16	12.9	77
17	14.0	65
18	10.6	63
19	11.4	74
20	12.8	77
21	13.0	46

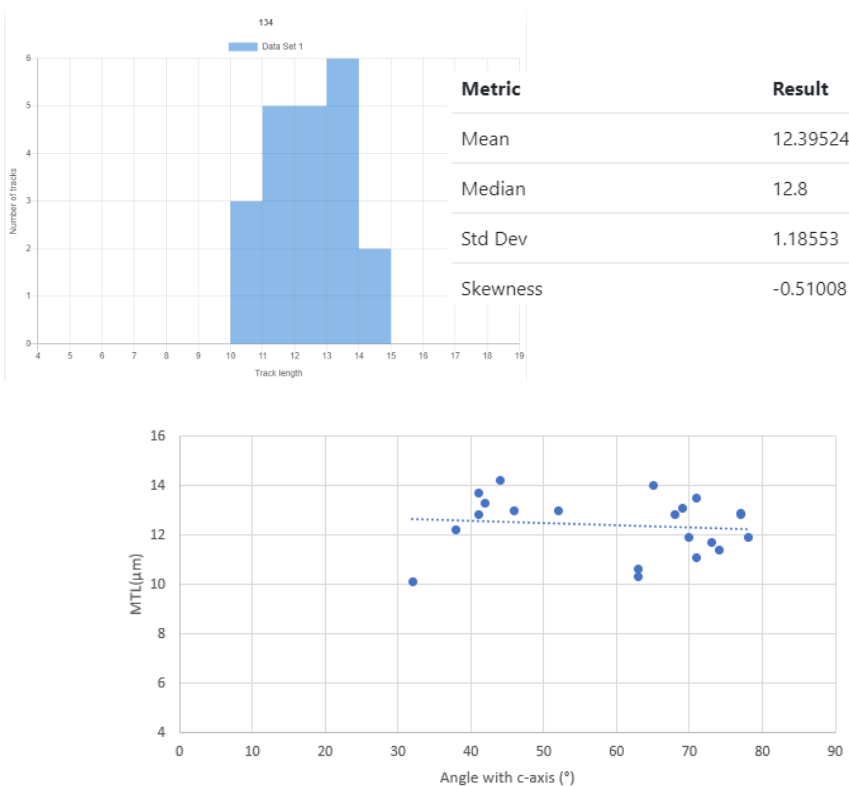
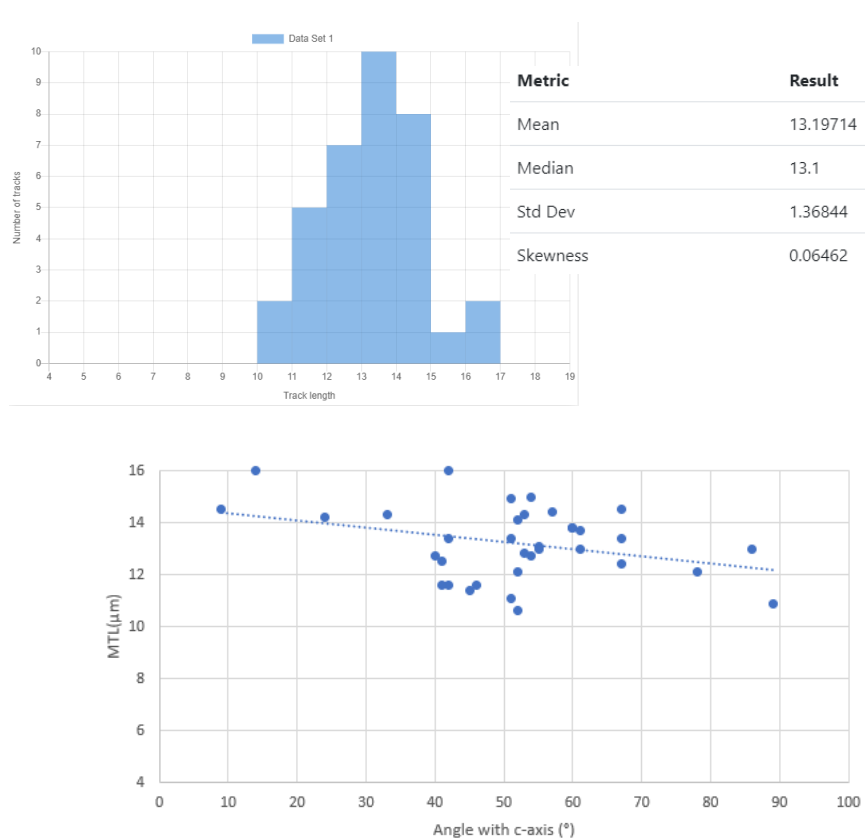


**Figure S.40.** Raw track lengths (L) in  $\mu\text{m}$  and angle with c-axis (A) for sample 135.

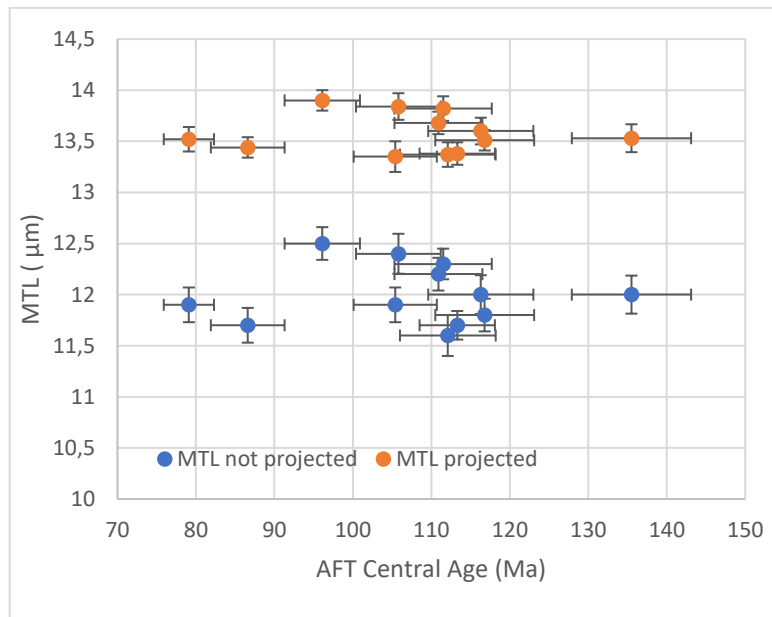
ID	L	A	ID	L	A
1	14.3	33	35	12.1	78
2	14.5	9	36		
3	14.2	24	37		
4	13.8	60	38		
5	10.9	89	39		
6	11.4	45	40		
7	14.4	57	41		
8	13.0	86	42		
9	13.8	60	43		
10	12.7	54	44		
11	12.5	41	45		
12	14.5	67	46		
13	11.6	46	47		
14	11.6	42	48		
15	14.1	52	49		
16	10.6	52	50		
17	13.4	51	51		
18	12.7	40	52		
19	11.6	41	53		
20	16.0	14	54		
21	11.1	51	55		
22	12.1	52	56		
23	15.0	54	57		
24	14.9	51	58		
25	13.4	67	59		
26	14.3	53	60		
27	13.7	61	61		
28	13.4	42	62		
29	13.1	55	63		
30	12.4	67	64		
31	12.8	53	65		
32	13.0	61	66		
33	16.0	42	67		
34	13.0	55	68		



### S3: Supporting graphs

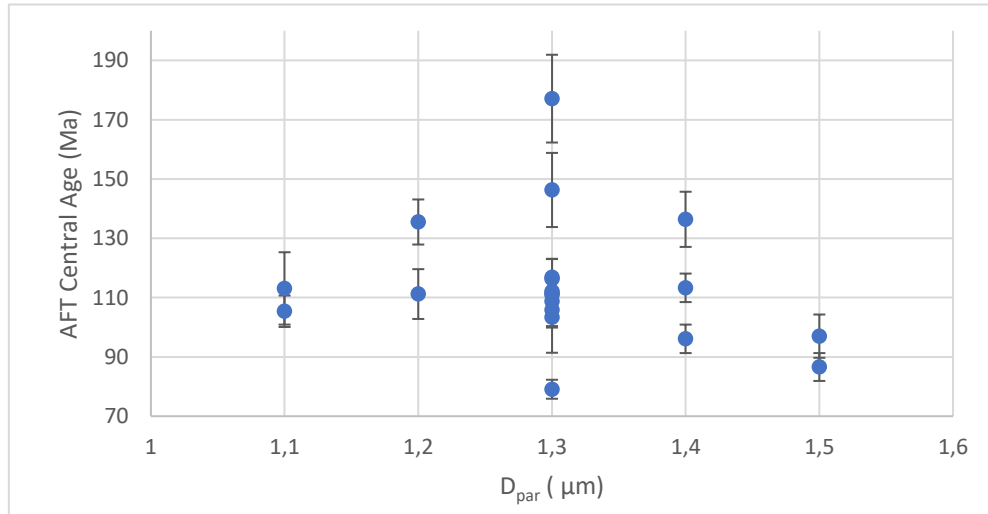
Graphs to investigate potential relationships between mean track length (MTL) and apatite fission track (AFT) central age, and AFT central age and  $D_{\text{par}}$ .

**Figure S.41.** MTL vs. AFT central age.



Sample	Central age	Err. Age	MTL	Err. MTL	MTL c-axis	Err. MTL c-axis
124	116.3	6.7	12.0	0.2	13.6	0.1
170	135.5	7.6	12.0	0.2	13.5	0.1
171	112.1	6.1	11.6	0.2	13.4	0.1
175	105.4	5.3	11.9	0.2	13.4	0.2
176	79.1	3.2	11.9	0.2	13.5	0.1
180	86.6	4.7	11.7	0.2	13.4	0.1
182	96.1	4.8	12.5	0.2	13.9	0.1
502	116.8	6.3	11.8	0.2	13.5	0.1
505	113.3	4.8	11.7	0.1	13.4	0.1
506	110.9	5.6	12.2	0.2	13.7	0.1
510	111.5	6.2	12.3	0.2	13.8	0.1
515	105.8	5.4	12.4	0.2	13.8	0.1

**Figure S.42.** AFT central age vs. mean  $D_{\text{par}}$ .



## S4: Modeling

Here we describe the modeling parameters we have used in QTQt (Gallagher, 2012). Details can be found in the paper.

### Modeling Strategies:

Modeling all samples separately:

- **M1:** C-axis projected lengths, constrained in one box ( $1250 \pm 50$  Ma;  $350 \pm 50$  °C), default priors. Present-day temperature set to  $30 \pm 5$  °C.

Modeling one representative samples (171):

- **M2:** C-axis projected lengths, constrained in one box ( $1250 \pm 50$  Ma;  $350 \pm 50$  °C), default priors. Present-day temperature set to  $30 \pm 5$  °C.
- **M3:** C-axis projected lengths, constrained in one box ( $1250 \pm 50$  Ma;  $350 \pm 50$  °C), wider priors ( $300 \pm 300$  Ma;  $150 \pm 150$  °C). Present-day temperature set to  $30 \pm 5$  °C.
- **M4:** C-axis projected lengths, constrained in two boxes ( $1250 \pm 50$  Ma;  $350 \pm 50$  °C and  $200 \pm 20$  Ma;  $200 \pm 20$  °C), default priors. Present-day temperature set to  $30 \pm 5$  °C.
- **M5:** C-axis projected lengths, constrained in two boxes ( $1250 \pm 50$  Ma;  $350 \pm 50$  °C and  $200 \pm 20$  Ma;  $50 \pm 5$  °C), default priors. Present-day temperature set to  $30 \pm 5$  °C.
- **M6:** No c-axis projected lengths, no constraints, default priors. Present-day temperature set to  $30 \pm 5$  °C.

Modeling ALL samples together:

- **M7:** C-axis projected lengths, constrained in one box ( $1250 \pm 50$  Ma;  $350 \pm 50$  °C), default priors. Present-day temperature set to  $30 \pm 5$  °C.
- **M8:** No c-axis projected lengths, constrained in one box ( $1250 \pm 50$  Ma;  $350 \pm 50$  °C), default priors. Present-day temperature set to  $30 \pm 5$  °C.

**Table S.1:** Table with result parameters of the modeling. According to Gallagher (2012) the acceptance rate for the time and temperature should be between ~20% and 60%, and the “birth” and “death” should have a similar value. The table show the values in green, if these conditions are reached. Ac: acceptance rates.

171	M2	M3	M4	M5	M6
Ac(Time)	0.5546	0.6214	0.6167	0.6560	0.6871
Ac(Temperature)	0.1741	0.1746	0.3378	0.2987	0.4129
Birth	0.0385	0.0236	0.0800	0.0766	0.2205
Death	0.4566	0.6483	0.0996	0.1668	0.2219
ALL together	Ac(Time)	Ac(temp.)	Birth	Death	
M7	0.3737	0.2688	0.0783	0.0774	
M8	0.3345	0.3150	0.0502	0.498	

### Why is acceptance rate important?

Acceptance rates in the context of modeling evaluation are crucial for several reasons. They serve as a metric for assessing the efficiency of proposed moves within the specified proposal time and temperature parameters in the modeling process. The acceptance rate, ideally targeted between approximately 20% to 60%, indicates the scale of the distribution for each model parameter from which iterative sampling occurs. This rate is essential as it ensures a balanced ratio between the addition (“birth”) and removal (“death”) of new t-T points, maintaining equilibrium within the model. By adjusting the proposal move values, one can observe a reciprocal effect on the acceptance rate. Modifying these values impacts the rate at which proposed iterations are accepted, thus influencing the overall efficiency of the model’s parameter sampling. Moreover, stability assessments of crucial metrics such as the log likelihood function (indicating data fit), posterior probability log, and the number of time-temperature points across iterations are pivotal. Stability in these metrics, as reflected in likelihood chains and acceptance rates, indicates that there are no discernible trends or significant value fluctuations across most iterations (Gallagher, 2012). This stability signifies a converged Markov Chain Monte Carlo (MCMC) simulation, a fundamental prerequisite for obtaining a reliable ensemble of accepted thermal histories that contribute to constructing the posterior distribution. In the context of research publications (Abbey et al., 2022), it is strongly encouraged to report the acceptance rates for the MCMC parameters. This reporting facilitates transparency and ensures reproducibility of the modeling process.

**Figure S.43:** Graphic results for every sample in modeling setting M1.

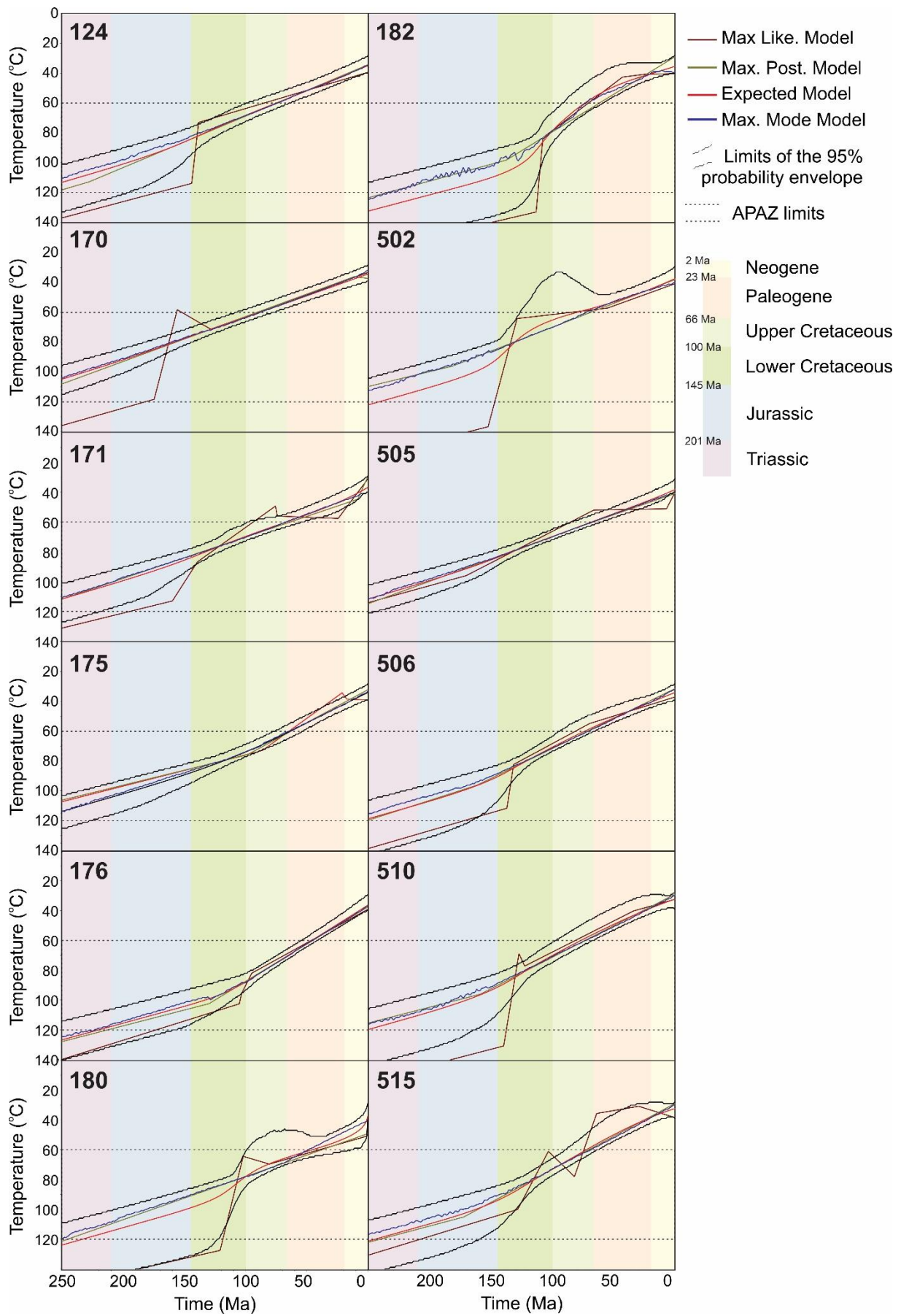


**Figure S.44:** Graphic results for sample 171 in modeling setting M2, M3, M4, M5, and M6.

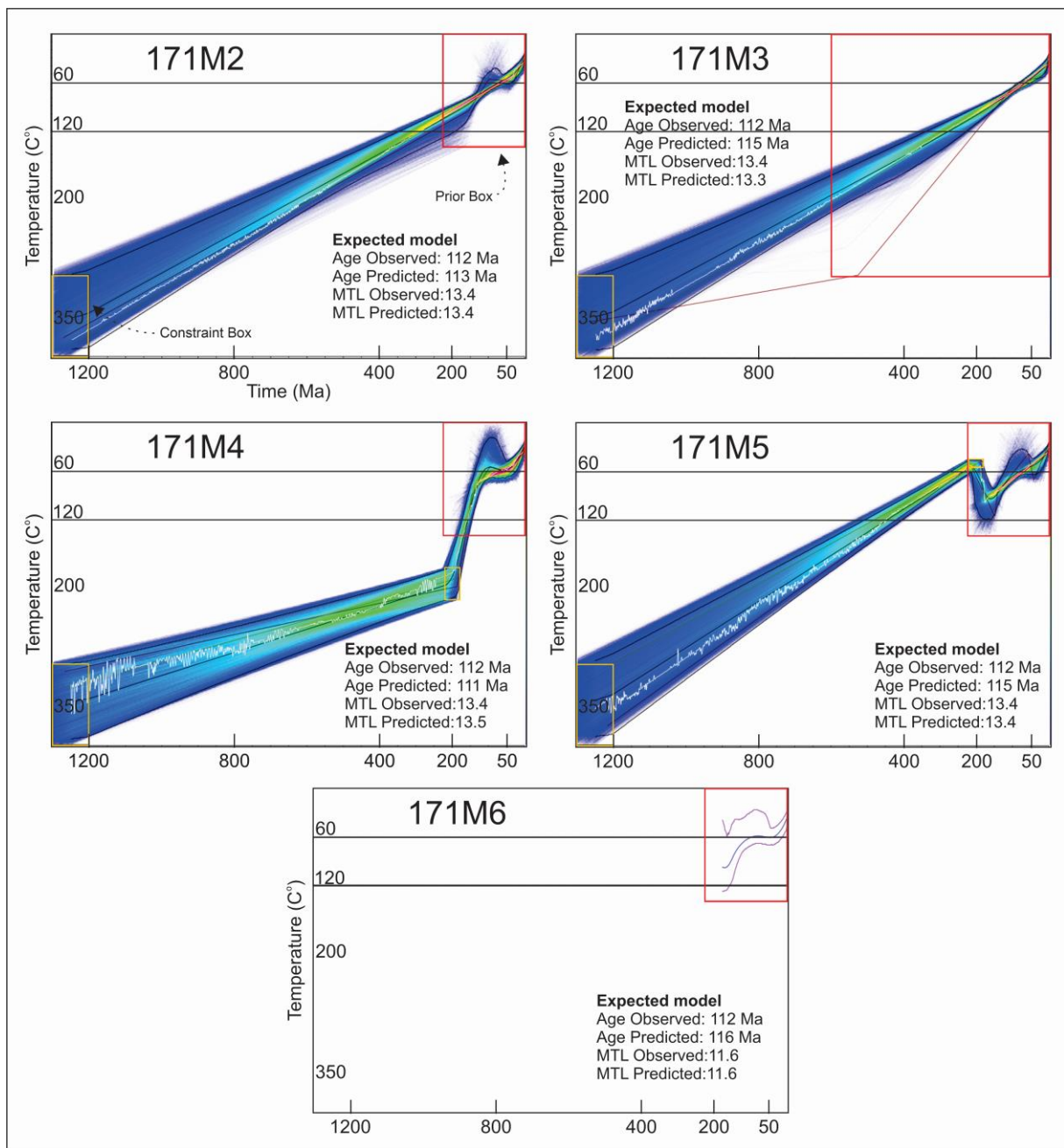


**Figure S.45:** Graphic results for all samples modeled together in setting M7. The graphs on the right display the relationship between Predicted and Observed ages, evaluating the model's performance in predicting ages compared to the actual recorded ages. 'Predicted age' refers to the estimated ages generated by the model, while 'Observed age' represents the true ages observed in the dataset. The scatter plot graphically represents each sample as points. In an ideal modeling scenario, perfect alignment between predicted and observed values forms a 45-degree straight line from the bottom left to the top right of the plot. Deviation from this line indicates disparities between predicted and observed ages, with points moving farther away implying greater differences between the model's predictions and the actual observed ages.

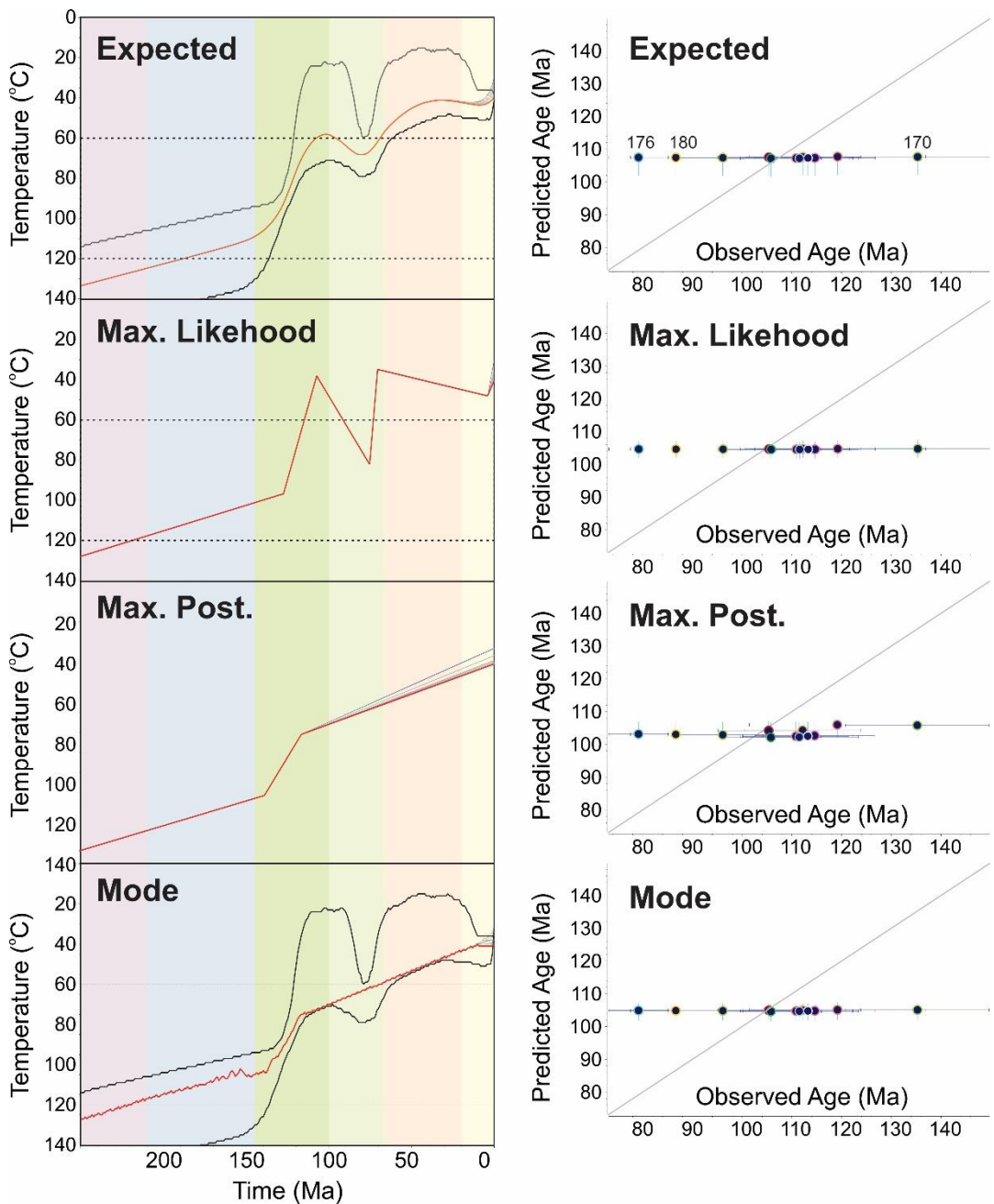


**Figure S.46:** Graphic results for all samples modeled together in setting M8. The graphs on the right display the relationship between Predicted and Observed ages, evaluating the model's performance in predicting ages compared to the actual recorded ages. 'Predicted age' refers to the estimated ages generated by the model, while 'Observed age' represents the true ages observed in the dataset. The scatter plot graphically represents each sample as points. In an ideal modeling scenario, perfect alignment between predicted and observed values forms a 45-degree straight line from the bottom left to the top right of the plot. Deviation from this line indicates disparities between predicted and observed ages, with points moving farther away implying greater differences between the model's predictions and the actual observed ages.

